IEEE Access
Multidisciplinary | Rapid Review | Open Access Journal

Date of publication xxxx 00, 0000, date of current version xxxx 00, 0000.

Digital Object Identifier 10.1109/ACCESS.2017.DOI

A Dynamics-Based Adaptive String Stable Controller for Connected Heavy Road Vehicle Platoon Safety

K. B. DEVIKA (Member, IEEE)[1], ROHITH G. (Member, IEEE)[2], VENKATA RAMANI SHREYA YELLAPANTULA [3] and SHANKAR C. SUBRAMANIAN (Senior Member, IEEE)[4]

[1,3,4]Department of Engineering Design, Indian Institute of Technology Madras, Chennai 600036, India
[2]Department of Mechanical Engineering, Indian Institute of Technology Gandhinagar, Gujarat 382355, India

Corresponding author: Shankar C. Subramanian (e-mail: shankarram@iitm.ac.in)

ABSTRACT This paper presents a string stable controller for the autonomous operation of a platoon of Heavy Commercial Road Vehicles (HCRVs) in a connected environment. This study considers factors such as brake/powertrain actuator dynamics, resistive forces, tyre model and wheel dynamics, which are crucial during on-road operation of HCRVs. A nonlinear vehicle dynamic model encompassing all these factors has been considered. The dependency between aerodynamic drag and inter-vehicular distance in the platoon has also been taken into account. The aforementioned factors motivated the use of Sliding Mode Control (SMC), which is a nonlinear and robust control technique. A lower level Proportional Integral Derivative (PID) controller has been successfully integrated with SMC to compensate for pneumatic brake and powertrain system delay. The designed controller was evaluated for string stable platoon operation by considering various road conditions, load conditions and operating speeds. It was observed that the string stable controller performance is highly dependent on the operating conditions. To ensure string stable operation for different operating scenarios, an adaptive time-headway based enhancement has also been integrated in the controller design. The efficacy of the proposed adaptive time-headway policy over the existing constant time-headway policy has been methodically analysed and a performance comparison between them has also been presented. The aspect of communication delay during connected vehicular operation has also been studied and the maximum tolerable communication delay magnitude for maintaining string stable operation has also been presented.

INDEX TERMS Actuation Dynamics, Heavy Commercial Road Vehicle, Platoon, String Stability, Sliding Mode Control, Vehicle Dynamics, Communication Delay

I. INTRODUCTION

A Heavy Commercial Road Vehicle (HCRV)[1] platoon is considered as an effective logistic solution due to attributes such as lower fuel consumption, reduced greenhouse gas emission and efficient utilization of available road infrastructure [1], [2]. Moreover, due to the increasing penetration of electrified vehicle technology, there has been renewed interest in platooning [3], [4], leading to the formulation and solution of numerous problems for safe, reliable and efficient platoon operations. The notion of string stability, defined in terms of inter-vehicular spacing, is of paramount interest for the practical realization of vehicle platoons [5]–[7]. Assuming the initial disturbances/perturbations to be bounded, if the spacing errors of all the vehicles are bounded uniformly in time, then the platoon is considered to be "string stable" [5], [6]. This is usually achieved by keeping the inter-vehicular spacing at a constant value, leading to a constant spacing policy [8], [9] or by allowing it to vary, but in a bounded manner, known as constant time-headway (CTH) policy [5], [10], [11]. For the autonomous operation of a vehicle platoon, a controller that could establish string stability is extremely important.

Most studies in this domain dealt with the realization of string stable controllers for passenger car platoons [12]–[18]. Moreover, they mostly relied on kinematic vehicle

[1]Heavy commercial road vehicles (such as trucks and buses) are also commonly referred to as heavy-duty commercial vehicles.

models for the design of controllers. However, while dealing with the practical realization of a high-speed vehicle platoon, it is imperative to include relevant crucial factors such as vehicle dynamics including aerodynamic drag and rolling resistance, tyre model, wheel dynamics, and brake/powertrain actuator dynamics during the platoon modelling and control design stages. Particularly in HCRV platoons, these factors are highly significant because of aspects such as pneumatic actuation delay, mass variation during laden and unladen operating conditions, and dynamic load transfer during braking. In a previous study [11], the importance of incorporating actuation dynamics and delays for the string stable controller design was analysed. It was observed that the pneumatic actuation delay in HCRVs is enough to deteriorate the performance of the string stable controller. But, the effects of wheel dynamics, tyre model and a complete dynamic vehicle model, that could further influence the controller performance, were not considered in that study. In this context, this paper demonstrates the importance of these factors for on-road HCRV string stable platoon operation and presents a more realistic controller design for the same. To ensure string stability in different road conditions, an adaptive time-headway policy for controller design is also presented.

An important aspect in platoon formation is the dependency of intervehicular spacing and the aerodynamic resistive forces, which determines the energy saving in platoon operation [19]–[21]. Since this dependency usually introduces nonlinearities into the platoon model [19], [22], it is usually neglected during string stable controller design. However, accurate modelling of drag interaction between vehicles is important to make the controller more effective and optimal. Behavior of aerodynamic drag coefficient during control action for longitudinal vehicle stability for car platoons has been analysed in [23]. This element has also been addressed in this work, by incorporating an adequate aerodynamic drag model.

All the aforementioned factors make an HCRV platoon model nonlinear. Also, a controller designed to establish the string stability should be robust enough to accommodate various disturbances arising from on-road operating conditions. Being a nonlinear and inherently robust control technique, Sliding Mode Controller (SMC) can be utilized in this regard. The research community has widely explored the suitability of SMC for the design of robust string stable controllers [8], [10], [14], [24]. However, while using SMC for practical control applications, chattering (high frequency control signal switching) has to be properly mitigated so as to prevent actuator damage [25]–[27]. Considering this aspect, most SMC based string stable controller designs available in the literature used boundary layer methods. However, boundary layer methods ensure chattering mitigation at the cost of finite time reachability and robustness [28], [29]. In this regard, this paper addresses this issue by using a recently proposed Power Rate Exponential Reaching Law (PRERL) for SMC design [30]. In addition to the property of chattering mitigation, PRERL is known for its advantages such as sufficient robustness, fast closed loop response and limited control action, which makes it an appropriate control strategy for string stable controller design [30].

As discussed, actuation delays in HCRVs can lead to string instability. To tackle string instability issues due to actuation delays, this work uses the Padé approximation based Proportional Integral Derivative (PID) based lower level controller, which enhances the performance of the actuation system by compensating actuation delay. Padé approximation method has been used to deal with actuator delays in vehicular platoons [31]–[34]. In this paper, the PID controller has been designed using Kharitonov approach to enhance its robustness. The lower level controller is designed to achieve the demanded wheel drive/brake torque to ensure string stability. The loss of string stability in the absence of a lower level controller has also been demonstrated in this paper.

The control action for string stable operation of a vehicle in the platoon depends on position and speed of neighbouring vehicles in the platoon. In a connected traffic environment these information are transmitted through wireless means that generally introduce transmission delays [35], [36]. Delays in reception/processing of information could adversely affect the platoon performance and might result in string instability. The effects of communication delay during data transmission in vehicular platoon environment have been discussed in the literature [37]–[39]. In this context, this paper also determines the maximum tolerable bound of communication delay in order to have a stable platoon operation for different on-road conditions. These values are then quantitatively compared for policies both with and without time-headway adaptation for different loading and road conditions.

A few relevant studies including experimental evaluation of heavy vehicle platooning are available in the literature [40]–[42]. In [40], a distributed approach using a network of controllers has been presented so as to maximize the amount of fuel saved by coordinating platoon formation. A detailed description on heavy vehicle platooning and the potential use of heavy vehicle platooning as a solution for sustainable freight transportation have been presented in [41]. This paper proposed vehicle layer control using cruise controller (CC) or adaptive cruise controller (ACC) and cooperative adaptive cruise controller (CACC) techniques. A cooperative look-ahead control (CLAC) framework for fuel-efficient and safe heavy-duty vehicle platoon operation has been presented in [42]. This design followed a dynamics-based approach and the efficacy of the controller was evaluated using simulation studies. Even though these papers demonstrated vehicle platooning via experimental evaluation and simulation studies, a methodical description of string stability controller design and lower level controller design by the inclusion of complete vehicle dynamics with wheel dynamics, tyre model and actuator dynamics was

This article has been accepted for publication in a future issue of this journal, but has not been fully edited. Content may change prior to final publication. Citation information: DOI 10.1109/ACCESS.2020.3039797, IEEE Access

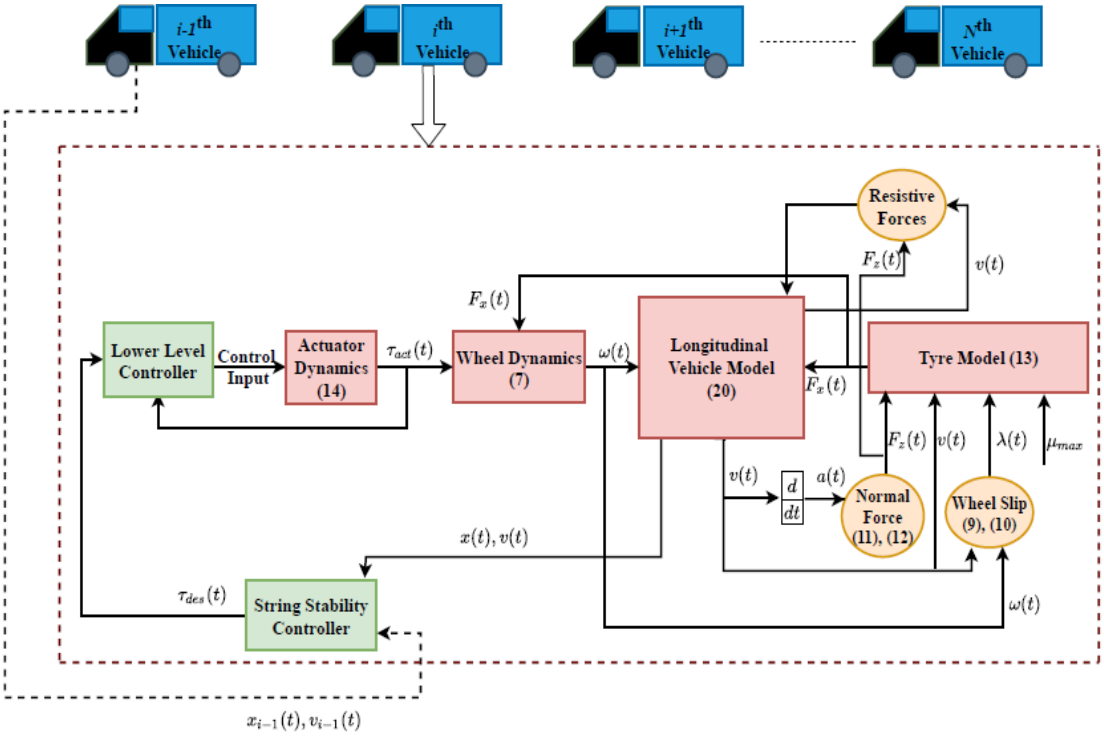

FIGURE 1: Overall Design Framework

not presented in them. Also, the effect of different road conditions on platoon stability has not been analysed.

Based on the above discussions, the major objective of the paper is to design a dynamics-based string stable controller for HCRV platoons. In this regard, specific tasks undertaken in this study include:

- The design of a string stable controller for HCRV platoon considering longitudinal vehicle dynamics, resistive forces, wheel dynamics, tyre model and actuation dynamics.
- The design of a lower level controller to enhance the actuation performance in HCRVs to ensure string stability.
- Ensure string stability in different road conditions through adaptive time-headway policy.
- Determine the maximum tolerable communication delay that guarantees string stability under different operating conditions.

II. PLATOON MODEL

The overall design framework of the HCRV platoon is presented in Fig. 1. The platoon consists of $N+1$ vehicles, with one leader and N followers. The assumptions made in this study are:

- The vehicles travel on a straight and flat road.
- Only longitudinal dynamics of the vehicle is considered.
- The tyre model parameters and vehicle parameters are assumed to be known.
- There is equal distribution of load on the left and right wheels of a specific axle of the vehicle.

The details of each component of the design framework (Fig. 1) are discussed below.

A. VEHICLE MODEL

The longitudinal motion of the leader vehicle is characterised by

$$\dot{x}_0(t) = v_0(t), \tag{1}$$

where, $x_0(t)$ and $v_0(t)$ are the position and longitudinal speed of the leader vehicle. The leader can be driven by a human or can be autonomous, and it can take action independent of the rest of the vehicles in the platoon. The longitudinal speed, $v_0(t)$ is the input from the leader vehicle that has to be followed by the follower vehicles. The free body diagrams showing the directions of forces on an individual follower vehicle during braking and drive mode are shown in Fig. 2 and 3. Now, the longitudinal motion of the follower vehicles is described by

$$\dot{x}_i(t) = v_i(t), \tag{2}$$

$$\dot{v}_i(t) = \frac{1}{m_i}(F_{xfi}(t) + F_{xri}(t) - F_{Ri}(t)), \tag{3}$$

where, $i = 1...N$.

The position and longitudinal speed of the follower vehicles are represented by $x_i(t)$ and $v_i(t)$ respectively. $F_{xfi}(t)$ and $F_{xri}(t)$ are the brake/traction force at the front and rear tyre-road interfaces, and m_i is the mass of the i^{th} vehicle

This article has been accepted for publication in a future issue of this journal, but has not been fully edited. Content may change prior to final publication. Citation information: DOI 10.1109/ACCESS.2020.3039797, IEEE Access

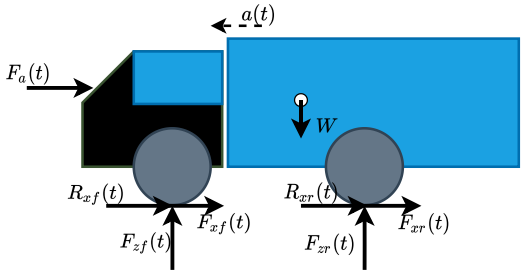

FIGURE 2: Individual follower vehicle free body diagram during braking.

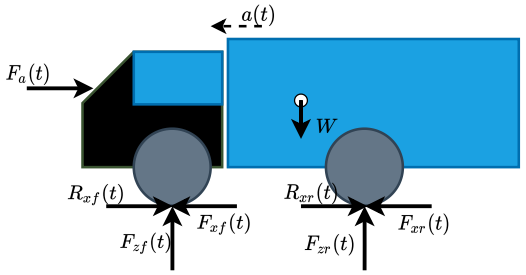

FIGURE 3: Individual follower vehicle free body diagram in drive mode.

in the platoon. $F_{Ri}(t)$ represents the resistive force on the i^{th} vehicle, which is given by

$$F_{Ri}(t) = F_{ai}(t) + R_{xfi}(t) + R_{xri}(t), \tag{4}$$

where, $F_{ai}(t)$ represents force due to aerodynamic drag, and R_{xfi} and R_{xri} are the forces due to rolling resistance at the front and rear wheels, respectively. The position and the longitudinal speed of the vehicle are measured with respect to its centre of gravity (C. G.) location.

1) Dependency Between Aerodynamic Drag and Intervehicular Distance

An advantage of platooning is the increase in fuel efficiency. While operating in a platoon formation, the aerodynamic drag associated with individual vehicles becomes less, resulting in a reduction in resistive forces, and hence increased fuel efficiency. Aerodynamic drag force for each vehicle is given by,

$$F_{ai}(t) = \rho\ a_{fi}\ C_{Di}(t)\frac{v_i(t)^2}{2}, \tag{5}$$

where, ρ is the density of air, $C_{Di}(t)$ is the aerodynamic drag coefficient and a_{fi} is the frontal area of the vehicle. For a homogeneous HCRV platoon, the frontal area is assumed to be same for each vehicle ($a_{fi} = a_f$). The drag coefficient of each vehicle in the platoon depends on the intervehicular distance $d_i(t)$, and in [19], the authors have presented a nonlinear relationship for the same, developed through empirical methods. This relationship is used in this work and is given as,

$$C_{Di}(t) = C_{D0}(\gamma_1 d_i(t)^{\gamma_2} + \gamma_3). \tag{6}$$

The drag coefficient of any individual vehicle (not operating in a platoon formation) is given as C_{D0}, and the parameters γ_1,γ_2, and γ_3 are obtained empirically [19].

2) Wheel Dynamics

The rotational dynamics of the wheels are given by

$$\begin{aligned} I_{fi}\dot{\omega}_{fi}(t) &= \tau_{fi}(t) - r_i F_{xfi}(t), \\ I_{ri}\dot{\omega}_{ri}(t) &= \tau_{ri}(t) - r_i F_{xri}(t), \end{aligned} \tag{7}$$

where, $i = 1...N$, and I_{fi} and I_{ri} are the moment of inertia of front and rear wheels, r_i is the tyre radius, $\tau_{fi}(t)$ and $\tau_{ri}(t)$ are the transmitted torques to the front and rear wheels respectively. On substituting for $F_{xfi}(t)$ and $F_{xri}(t)$ from (7) in (3), one can obtain the follower vehicle dynamics as,

$$\begin{aligned} \dot{v}_i(t) =& \frac{1}{m_i}\Bigg[\frac{1}{r_i}(\tau_{fi}(t) - I_{fi}\dot{\omega}_{fi}(t)) + \frac{1}{r_i}(\tau_{ri}(t) - I_{ri}\dot{\omega}_{ri}(t)) \\ & - F_{Ri}(t)\Bigg]. \end{aligned} \tag{8}$$

3) Tyre Model

The longitudinal forces at the tyre-road interface depend on the longitudinal slip ratios (λ_f, λ_r), the normal load on the tyre (F_{zf}, F_{zr}) and the friction coefficient (μ) between the tyres and the ground [43].

The longitudinal slip ratio per wheel during braking is defined as,

$$\lambda(t) = \frac{v(t) - r\ \omega(t)}{v(t)}, \tag{9}$$

and during acceleration,

$$\lambda(t) = \frac{r\ \omega(t) - v(t)}{r\ \omega(t)}, \tag{10}$$

where, r represents the tyre radius and $\omega(t)$ represents angular speed of the wheel.

The normal load on the tyre is determined by the total weight of the vehicle, C.G. location, longitudinal acceleration of the vehicle, aerodynamic drag forces and road inclination. Considering these factors and neglecting the road inclination angle, the normal forces on both front and rear tyres of the i^{th} vehicle in the platoon are given by,

$$F_{zfi}(t) = \frac{mgl_r - F_{ai}(t)\ h_a - ma_i(t)h_{cg}}{l_f + l_r}, \tag{11}$$

$$F_{zri}(t) = \frac{mgl_f + F_{ai}(t)\ h_a + ma_i(t)h_{cg}}{l_f + l_r}, \tag{12}$$

where, $a_i(t)$ is the longitudinal acceleration, h_{cg} is the height of the C.G. of the vehicle, h_a is the height of the location at which the equivalent aerodynamic force acts and

This article has been accepted for publication in a future issue of this journal, but has not been fully edited. Content may change prior to final publication. Citation information: DOI 10.1109/ACCESS.2020.3039797, IEEE Access

l_f and l_r are the longitudinal distance of the front axle and rear axle from the C.G. of the vehicle.

For a wide range of operating conditions, the Magic Formula (MF) tyre model [44] gives a good representation of forces acting on the tyre-road interface and is used in this work. Using the MF model, for a single wheel, the longitudinal force can be represented as,

$$F_x(\lambda(t)) = D\sin(C\tan^{-1}(B\lambda_x - E(B\lambda_x(t) - \tan^{-1} B\lambda_x(t)))) + S_V, \quad (13)$$

where, $\lambda_x(t) = \lambda(t) + S_H$.
In this work, the MF model parameters, B, C, D, E, S_H, S_V were obtained from the vehicle dynamic simulation software, IPG TruckMaker®. The parameter B represents the stiffness factor, which determines the slope at the origin of the force curve as presented by (13). The shape factor C controls the shape of the curve and the parameter E is used to control the shape and horizontal position of the peak. The parameter D represents the peak factor. The parameters S_H and S_V represent the horizontal and vertical shifts in the force curve respectively, predominantly due to ply-steer and conicity effects. The parameters B, C, E, and S_H are dimensionless parameters, and the parameters D and S_V have the dimension of force [44].

From the block diagram shown in Fig. 1, it can be understood that the force component $F_x(t)$ calculated by the tyre model is provided to the wheel dynamics block that calculates the angular speed $\omega(t)$. Using this angular speed $\omega(t)$, the force component $F_x(t)$ (calculated by the tyre model) and the resistive forces, the vehicle model computes the position and longitudinal speed. This information is used by the string stability controller (sliding mode controller) to synthesise the desired torque input for string stable platoon operation.

B. ACTUATION MODEL

The air brake system is commonly used in HCRVs and it uses compressed air as the operating medium for actuation. The dynamic response of the air brake depends upon factors such as compressibility of air, pipe lengths and valve response time. All these factors result in a significant time delay in the brake system response. Further, there is a significant time taken for air pressure build up in the brake actuator. These physical phenomena motivated the use of the time delay (T_d) and the time constant (τ_d) while modelling the brake response. By conducting Hardware in Loop experiments for a wide range of operating conditions and through frequency domain and time domain analysis, Sridhar et al. characterised the air brake system using a first order process with time delay [45], whose transfer function is given by,

$$P(s) = \frac{\tau(s)}{\tau_{des}(s)} = \frac{1}{1+\tau_d s} e^{-T_d s}, \quad (14)$$

where, τ_{des} and τ represent the demanded brake torque and actual brake torque developed. This model has been used in this study to characterise actuation system dynamics. In [45], the specific values for time constant (τ_d) and time delay (T_d) have also been experimentally obtained as $\tau_d = 260$ ms and $T_d = 45$ ms. These values have been utilized in this work. From literature, it can be seen that the acceleration/drive phase dynamics can also be approximated as first order models with time constants and delays [46]. Hence, for the analysis of the effect of powertrain dynamics during acceleration/drive phases, a similar model was used. From literature, it was also found that, $\tau_d = 260$ ms and $T_d = 45$ ms are feasible values of time constant and time delay for actuation dynamics during braking as well as acceleration/drive phases [46]. These values were hence used for incorporating actuation dynamics in the platoon framework.

C. VEHICULAR SPACING MODEL

The spacing between a pair of vehicles in the platoon is given by

$$d_i(t) = x_{i-1}(t) - x_i(t). \quad (15)$$

The desired inter-vehicular distance is defined as

$$s_d(t) = s_o + h_i v_i(t), \quad (16)$$

where, s_o and h_i represent standstill spacing and the time-headway respectively.
Spacing error between two consecutive vehicles is given by

$$e_i(t) = d_i(t) - s_d(t). \quad (17)$$

To avoid collision between two consecutive vehicles, the objective is to drive the spacing error between the vehicles to zero, such that the desired intervehicular distance is always maintained. Hence, the control objective is to make:

$$d_i(t) = s_o + h_i v_i(t), \quad (18)$$
$$v_i(t) = v_0(t). \quad (19)$$

During the perturbation maneuver, the controller makes the follower vehicles to follow the longitudinal speed of the leader vehicle ($v_o(t)$) and always tries to maintain the desired spacing of $S_d(t)$ between the vehicles so that collision is avoided. Once the leader vehicle comes back to the normal steady state speed (nominal platoon speed), the controller makes the follower vehicle to reach and follow the same.

III. STRING STABLE CONTROLLER

For the design of string stable controller, it is assumed that the same type of brake actuator is present in the front and rear wheels. During drive mode, $\tau_f(t) = 0$, $\tau_r(t) = \tau(t)$ (rear wheel drive), and during braking mode, it is assumed that $\tau_f(t) = \tau_r(t) = \tau(t)$. Hence, (8) (which was obtained

This article has been accepted for publication in a future issue of this journal, but has not been fully edited. Content may change prior to final publication. Citation information: DOI 10.1109/ACCESS.2020.3039797, IEEE Access

by substituting for $F_{xfi}(t)$ and $F_{xri}(t)$ from (7) in (3)) becomes,

$$\dot{v}_i(t) = \begin{cases} \frac{1}{m_i r_i}\tau_i(t) - \frac{1}{m_i r_i}\left[I_{fi}\dot{\omega}_{fi}(t) + I_{ri}\dot{\omega}_{ri}(t)\right] - \\ \qquad \frac{F_{Ri}(t)}{m_i}, \qquad \text{during drive mode,} \\ \frac{2}{m_i r_i}\tau_i(t) - \frac{1}{m_i r_i}\left[I_{fi}\dot{\omega}_{fi}(t) + I_{ri}\dot{\omega}_{ri}(t)\right] - \\ \qquad \frac{F_{Ri}(t)}{m_i}, \qquad \text{during brake mode.} \end{cases} \tag{20}$$

For simplicity, the above expressions are written in the following form:

$$\dot{v}_i(t) = \Gamma + \Lambda u_i(t), \tag{21}$$

where, $\Gamma = -\frac{1}{m_i r_i}(I_{fi}\dot{\omega}_{fi}(t) + I_{ri}\dot{\omega}_{ri}(t)) - \frac{F_{Ri}(t)}{m_i}$, $\Lambda = \frac{1}{m_i r_i}$ (drive mode), $\Lambda = \frac{2}{m_i r_i}$ (brake mode) and $u_i(t) = \tau_i(t)$.

For the design of PRERL based SMC, the following sliding function was chosen [10]:

$$s_i(t) = e_i(t) + \int_0^t \kappa e_i(\tau)d\tau, \tag{22}$$

where, $e(t)$ represents the intervehicular spacing error given by (17). The term, κ is a positive constant that represents the slope of the sliding function. The integral term in the sliding function subdues the need for derivative of acceleration (jerk) data from preceding vehicles (if the standard sliding function, $s_i(t) = \dot{e}_i(t) + \kappa e_i(t)$ were chosen, jerk terms would appear while obtaining the control equation by taking the first derivative of the sliding function and this additional data requirement makes the controller design complex and subsequently makes controller implementation difficult).

This sliding function has been chosen for driving the intervehicular spacing error between two consecutive vehicles to zero. In order to guarantee string stability, the sliding function was further redefined such that the propagation of spacing error is reduced along the platoon [10]. The new sliding function is given by

$$S_i(t) = \begin{cases} qs_i(t) - s_{i+1}(t), & i = 1, ..., N-1 \\ qs_i(t), & i = N \end{cases}, \tag{23}$$

where, q>0.

Now, consider the PRERL structure given by

$$\dot{S}_i(t) = -\frac{G}{\delta_0 + (1-\delta_0)e^{-\alpha|S_i(t)|^p}}|S_i(t)|^\beta \text{sign}(S_i(t)), \tag{24}$$

where $G > 0$ is the controller gain, $\delta_0 < 1, \alpha > 0, 0 < \beta < 0.5$ and $p > 0$ are controller parameters that affect the reaching time and chattering mitigation properties. Now, evaluating the first derivatives of (23) and (22) and using (21) and (24),

$$\begin{aligned} \dot{S}_i(t) &= q(v_{i-1}(t) - v_i(t)) + q\kappa e_i(t) - \dot{e}_{i+1}(t) - \kappa e_{i+1}(t) \\ &\quad - qh_i\Gamma - qh_i\Lambda u_i(t) \\ &= -\frac{G}{\delta_0 + (1-\delta_0)e^{-\alpha|S_i(t)|^p}}|S_i(t)|^\beta \text{sign}(S_i(t)), \\ &\qquad\qquad i = 1, ..., N-1, \end{aligned} \tag{25}$$

$$\begin{aligned} \dot{S}_N(t) &= q(v_{i-1}(t) - v_i(t)) + q\kappa e_N(t) - qh_N\Gamma \\ &\quad - qh_N\left[\frac{1}{m_i r_i}f_f\left(1 + \frac{\beta}{1-\beta}\right)\right]u_i(t) \\ &= -\frac{G}{\delta_0 + (1-\delta_0)e^{-\alpha|S_N(t)|^p}}|S_N(t)|^\beta \text{sign}(S_N(t)), \end{aligned} \tag{26}$$

from which the torque control input, $u_i(t) = \tau_i(t)$ can be obtained as

$$\begin{aligned} \tau_i(t) = &\frac{-1}{qh_i\Lambda}\left[\frac{-G}{\delta_0 + (1-\delta_0)e^{-\alpha|S_i(t)|^p}}|S_i(t)|^\beta \text{sign}(S_i(t))\right. \\ &- q(v_{i-1}(t) - v_i(t)) - q\kappa e_i(t) + \dot{e}_{i+1}(t) + \kappa e_{i+1}(t) \\ &\left. + qh_i\Gamma\right], \qquad\qquad i = 1, ..., N-1, \end{aligned} \tag{27}$$

and for the last vehicle in the platoon,

$$\begin{aligned} \tau_N(t) = &\frac{-1}{qh_N\Lambda}\left[\frac{-G}{\delta_0 + (1-\delta_0)e^{-\alpha|S_N(t)|^p}}|S_N(t)|^\beta \text{sign}(S_N(t))\right. \\ &\left. - q(v_{N-1}(t) - v_N(t)) - q\kappa e_i(t) + qh_N\Gamma\right]. \end{aligned} \tag{28}$$

For ensuring the notion of string stability in a platoon, the controller should act such that the spacing error between a pair of vehicles should be attenuated in the event of any bounded perturbations and shall not aggravate along the platoon.

Proposition 1. *If the disturbance magnitude, $|D(t)|$ acting on an individual vehicle is within the bound, $|D(t)| < \frac{G|S_i(t)|^\beta}{(\delta_0 + (1-\delta_0)e^{-\alpha|S_i(t)|^p})qh_i}$, spacing error between two consecutive vehicles asymptotically tends to zero in finite time.*

Proof. In order to ensure the stability with respect to (23), consider a Lyapunov function as

$$V_i(t) = \frac{1}{2}S_i(t)^2. \tag{29}$$

Differentiating (29) gives,

$$\dot{V}_i(t) = S_i(t)\dot{S}_i(t). \tag{30}$$

Considering a bounded disturbance $D(t)$ in (21), from (23) the first derivative of the sliding function $S_i(t)$ can be obtained as

$$\begin{aligned}\dot{S}_i(t) =& q(v_{i-1}(t) - v_i(t)) + q\kappa e_i(t) - \dot{e}_{i+1}(t) - \kappa e_{i+1}(t) \\ & - qh_i(\Gamma + \Lambda u_i(t) + D(t)).\end{aligned} \tag{31}$$

Substituting (31) in (30),

$$\begin{aligned}\dot{V}_i(t) =& S_i(t)\big(q(v_{i-1}(t) - v_i(t)) + q\kappa e_i(t) - \dot{e}_{i+1}(t) \\ & - \kappa e_{i+1}(t) - qh_i(\Gamma + \Lambda u_i(t) + D(t))\big).\end{aligned} \tag{32}$$

Substituting the PRERL based control equation (27) in the above equation,

$$\begin{aligned}\dot{V}_i(t) =& \frac{-S_i(t)G}{\delta_0 + (1-\delta_0)e^{-\alpha|S_i(t)|^p}}|S_i(t)|^\beta \text{sign}(S_i(t)) \\ & - S_i(t)qh_iD(t).\end{aligned} \tag{33}$$

According to Lyapunov stability condition, for asymptotic stability of the equilibrium state, $\dot{V}_i(t) < 0, \forall\ S_i(t) \neq 0$.

When, $S_i(t) > 0$, the condition for establishing asymptotic stability can be obtained from (33) as,

$$\dot{V}_i(t) = \frac{-S_i(t)G}{\delta_0 + (1-\delta_0)e^{-\alpha|S_i(t)|^p}}|S_i(t)|^\beta - S_i(t)qh_iD(t) < 0, \tag{34}$$

which gives,

$$D(t) > \frac{-G|S_i(t)|^\beta}{(\delta_0 + (1-\delta_0)e^{-\alpha|S_i(t)|^p})qh_i}. \tag{35}$$

When, $S_i(t) < 0$, the condition for establishing asymptotic stability can be obtained from (33) as,

$$\dot{V}_i(t) = \frac{-S_i(t)G}{\delta_0 + (1-\delta_0)e^{-\alpha|S_i(t)|^p}}|S_i(t)|^\beta + S_i(t)qh_iD(t) < 0, \tag{36}$$

which gives,

$$D(t) < \frac{G|S_i(t)|^\beta}{(\delta_0 + (1-\delta_0)e^{-\alpha|S_i(t)|^p})qh_i}. \tag{37}$$

Hence for ensuring asymptotic stability, the bound on the perturbation is (using (42) and (44)),

$$|D(t)| < \frac{G|S_i(t)|^\beta}{(\delta_0 + (1-\delta_0)e^{-\alpha|S_i(t)|^p})qh_i}. \tag{38}$$

□

Proposition 1 provides an idea of how much bounded disturbance the system can handle, if the platoon were perturbed away from the string stable condition. If one were to use this approach in practice to select a specific set of design parameters (controller parameters, time-headway, and intervehicular spacing), then using proposition 1, one can be informed about the acceleration/deceleration disturbance limit that the system can handle. The variable $S_i(t)$ in Proposition 1 essentially carries the information regarding the intervehicular spacing errors, $e_i(t) = d_i(t) - s_d(t)$, where, $d_i(t)$ is the spacing between a pair of vehicles, and $s_d(t)$ is the desired inter-vehicular distance. It is logical to assume that the magnitude of $e_i(t)$ (and hence the magnitude of $S_i(t)$) impacts the maximum allowable acceleration/deceleration disturbance, $|D(t)|$. So, during real-time implementation, if one is able to obtain the magnitude of $e_i(t)$, then one can have a better idea about the limits of $|D(t)|$ on the platoon stability.

A. COMPARISON WITH CONVENTIONAL SMC STRUCTURE

The term $|S_i(t)|$ is present in the above condition owing to the structure of the PRERL based controller. If one were to opt for constant rate reaching law based SMC design ($G\text{sign}(S_i(t))$), which is a conventional SMC design approach [47], then, the expression would become $|D(t)| < G/qh_i$. Then, one could observe that the requirement on $|D(t)|$ is not dependent on $S_i(t)$. But this is at the expense of high frequency control signal switching, an inherent disadvantage of constant rate reaching law based SMC design, which restricts its practical utility.

To clarify this point, the stability analysis using constant rate reaching law based SMC design is presented below.

Constant rate reaching law is given by [47]:

$$\dot{S}_i(t) = -G\text{sign}(S_i(t)), \tag{39}$$

where, $G > 0$. On using control equation based on above constant rate reaching law structure (similar to (27)), equation (33) can be written as,

$$\dot{V}_i(t) = -S_i(t)G\text{sign}(S_i(t)) - S_i(t)qh_iD(t). \tag{40}$$

According to Lyapunov stability condition, for asymptotic stability of the equilibrium state, $\dot{V}_i(t) < 0, \forall\ S_i(t) \neq 0$.

When, $S_i(t) > 0$, the condition for establishing asymptotic stability can be obtained from equation (40) as,

$$\dot{V}_i(t) = -S_i(t)G - S_i(t)qh_iD(t) < 0, \tag{41}$$

which gives,

$$D(t) > \frac{-G}{qh_i}. \tag{42}$$

When, $S_i(t) < 0$, the condition for establishing asymptotic stability can be obtained from equation (40) as,

$$\dot{V}_i(t) = -S_i(t)G + S_i(t)qh_iD(t) < 0, \tag{43}$$

which gives,

$$D(t) < \frac{G}{qh_i}. \tag{44}$$

Hence, for ensuring asymptotic stability, the bound on the perturbation is (using conditions (42) and (44)),

$$|D(t)| < \frac{G}{qh_i}. \tag{45}$$

Thus, the stability condition using conventional constant rate reaching law based SMC does not have dependence between disturbance magnitude $|D(t)|$ and sliding function $S_i(t)$.

This article has been accepted for publication in a future issue of this journal, but has not been fully edited. Content may change prior to final publication. Citation information: DOI 10.1109/ACCESS.2020.3039797, IEEE Access

However, this constant rate reaching law has the disadvantage of control signal chattering [47]. While using SMC for practical control applications, chattering (high frequency control signal switching) has to be properly mitigated so as to prevent actuator damage.

B. STRING STABILITY CONDITION

To analyse the notion of string stability using the presented SMC design, consider the error propagation transfer function [10],

$$G_i(s) = \frac{E_{i+1}(s)}{E_i(s)}, \tag{46}$$

where, $E_i(s)$ and $E_{i+1}(s)$ denote the Laplace transform of spacing error propagation between consecutive pair of vehicles in the platoon. For string stability [10],

$$\left|\left|G_i(s)\right|\right| < 1 \quad \forall\ i = 1, ..., N. \tag{47}$$

The asymptotic stability of spacing error between pair of vehicles using PRERL has already been established, which ensures,

$$S_i(t) = 0, \tag{48}$$

in finite time. Hence, based on (23),

$$qs_i = s_{i+1}. \tag{49}$$

Now, using (22),

$$q\big(e_i(t) + \int_0^t \kappa e_i(\tau)d\tau\big) = e_{i+1}(t) + \int_0^t \kappa e_{i+1}(\tau)d\tau. \tag{50}$$

On taking Laplace transform on both sides,

$$q\big[E_i(s) + \frac{\kappa}{s}E_i(s)\big] = E_{i+1}(s) + \frac{\kappa}{s}E_{i+1}(s), \tag{51}$$

which gives the spacing error propagation transfer function as,

$$G_i(s) = \frac{E_{i+1}(s)}{E_i(s)} = q. \tag{52}$$

Since, for string stability, $\left|\left|G_i(s)\right|\right| < 1$, by selecting the parameter range, $0 < q < 1$, the presented controller design framework would ensure string stable platoon operation.

Remark 1. In an ideal scenario, the string stability condition given by (47) should hold for all frequencies [10]. The prevalence of using a kinematic model to realize platoon operations in the literature also suggested the same [10]. But, the consideration of actuator dynamics puts a restriction on the achievable acceleration/deceleration values. For example, in practice, once the brake is applied, there would be a minimum time for the brake pressure to increase and generate the braking force. This effect has been characterised by a first order plus time delay model given as by (14). Even in an otherwise ideal scenario of having the braking action as soon as the pressure develops, i.e., zero time delay ($T_d = 0$), the achievable acceleration/deceleration is still limited by the actuator system dynamics (characterised by the time constant). Considering such a scenario,

$$P(s) = \frac{1}{1 + \tau_d s}, \tag{53}$$

which, on replacing s by $j\omega$ gives,

$$P(j\omega) = \frac{1}{1 + j\tau_d\omega}. \tag{54}$$

This can be written as,

$$P(j\omega) = \frac{1}{1 + j\omega/\omega_{cd}}, \tag{55}$$

where, ω_{c_d} is the cut-off frequency and for $\tau_d = 260$ ms,

$$\omega_{c_d} = 1/\tau_d = 1/0.26 = 3.85 \text{ Hz}. \tag{56}$$

From the actuator dynamics, the value of cut-off frequency is found to be ω_{c_d} = 3.85 Hz. For frequencies above this value, the actuator cannot respond properly since the command signal would exceed its bandwidth. Hence, for perturbations having frequencies above this bandwidth, owing to the actuator dynamics, a string stable operation could not be achieved for the class of vehicles considered in this study.

C. LOWER LEVEL CONTROLLER

Actuation system delay in HCRVs platoon can lead to string instability during platoon operation [11]. Hence, the response characteristics of HCRV's actuation system (described by (14)) is improved by using a lower level controller. The presence of the time delay term in the system transfer function (14) makes it an improper transfer function. Hence, Padé approximation has been used [48] to obtain a proper transfer function. Using first order Padé approximation, the actuation model (14) can be rewritten as

$$P(s) \approx \frac{(2 - T_d s)}{(1 + s\tau_d)(2 + T_d s)}. \tag{57}$$

On augmenting the actuation system with a lower level controller, the closed-loop transfer function becomes

$$\frac{\tau(s)}{\tau_{des}(s)} = \frac{C(s)P(s)}{1 + C(s)P(s)}, \tag{58}$$

where, $C(s)$ represents the transfer function of the controller. A PID controller is used here, whose transfer function is given by

$$C(s) = K_p + \frac{K_i}{s} + K_d s. \tag{59}$$

Here, K_p, K_i and K_d are the proportional, integral and derivative gains respectively.

In practice, the parameters of the actuator such as, time constant (τ_d) and time delay (T_d) are subjected to variations due to varying operating conditions and aging of the actuator. Hence, the controller should possess sufficient robustness towards parametric variations. In this regard, the PID controller tuning has been done based on Kharitonov's

This article has been accepted for publication in a future issue of this journal, but has not been fully edited. Content may change prior to final publication. Citation information: DOI 10.1109/ACCESS.2020.3039797, IEEE Access

theorem, such that the controller is robust with respect to deterministic bounded parametric uncertainties [49]. Based on (57), (58) and (59), the closed loop transfer function of the actuation system can be obtained as

$$\frac{\tau(s)}{\tau_{des}(s)} = \frac{(K_p s + K_i + K_d s^2)(2 - T_d s)}{As^3 + Bs^2 + Cs + D}, \tag{60}$$

where, $A = T_d\tau_d - K_d T_d$, $B = T_d + 2\tau_d + 2K_d - K_p T_d$, $C = 2 + 2K_p - K_i T_d$ and $D = 2K_i$.
For robust PID controller design, the Kharitonov's polynomials can be realized as follows [49]:

$$\begin{aligned} K^1(s) &= \underline{\delta}_0 + \underline{\delta}_1 s + \overline{\delta}_2 s^2 + \overline{\delta}_3 s^3 \\ K^2(s) &= \underline{\delta}_0 + \overline{\delta}_1 s + \overline{\delta}_2 s^2 + \underline{\delta}_3 s^3 \\ K^3(s) &= \overline{\delta}_0 + \underline{\delta}_1 s + \underline{\delta}_2 s^2 + \overline{\delta}_3 s^3 \\ K^4(s) &= \overline{\delta}_0 + \overline{\delta}_1 s + \underline{\delta}_2 s^2 + \underline{\delta}_3 s^3, \end{aligned} \tag{61}$$

where the Kharitonov's coefficients are,
$\delta_0 \in [\underline{\delta}_0, \overline{\delta}_0] = [2K_i, 2K_i]$,
$\delta_1 \in [\underline{\delta}_1, \overline{\delta}_1] = [2 + 2K_p - K_i T_{d_{min}}, 2 + 2K_p - K_i T_{d_{max}}]$,
$\delta_2 \in [\underline{\delta}_2, \overline{\delta}_2] = [T_{d_{min}} + 2\tau_{min} + 2K_d - K_p T_{d_{min}}, T_{d_{max}} + 2\tau_{max} + 2K_d - K_p T_{d_{max}}]$,
$\delta_3 \in [\underline{\delta}_3, \overline{\delta}_3] = [T_{d_{min}}\tau_{d_{min}} - K_d T_{d_{min}}, T_{d_{max}}\tau_{d_{max}} - K_d T_{d_{max}}]$.
The subscripts min and max indicate the bounds on uncertainties in the parameters, T_d and τ_d, assuming the uncertainties to be deterministic. According to Kharitonov's theorem, for robust stability, all the above four Kharitonov's polynomials should be Hurwitz [49]. On applying the necessary and sufficient conditions for Hurwitz stability to the four polynomials, the following inequalities were obtained:
$\underline{\delta}_0 > 0, \overline{\delta}_0 > 0,\ \underline{\delta}_1 > 0,\ \overline{\delta}_1 > 0,\ \underline{\delta}_2 > 0,\ \overline{\delta}_2 > 0,\ \underline{\delta}_3 > 0,\ \overline{\delta}_3 > 0,$
$\overline{\delta}_2\underline{\delta}_1 > \overline{\delta}_3\underline{\delta}_0,\ \overline{\delta}_1\overline{\delta}_2 > \underline{\delta}_3\underline{\delta}_0,\ \underline{\delta}_1\underline{\delta}_2 > \overline{\delta}_3\overline{\delta}_0,\ \underline{\delta}_2\overline{\delta}_1 > \underline{\delta}_3\overline{\delta}_0$.
For the robust operation of HCRV actuation system, the gains, K_p, K_i and K_d should be selected such that the above inequalities are satisfied.

IV. PERFORMANCE EVALUATION OF THE STRING STABLE CONTROLLER

The designed string stable controller has been evaluated for the following vehicle conditions and on-road scenarios.

- Each vehicle was considered to have a full laden mass of 16200 kg and an unladen mass of 4700 kg.
- The platoon has been evaluated for road surfaces with different tyre-road friction coefficients (μ). Operation on roads with high μ ($\mu = 0.8$), middle μ ($\mu = 0.5$) and low μ ($\mu = 0.3$) were evaluated.
- The controller was evaluated for a high operating speed (15 m/s) and a low operating speed (5 m/s).

A pictorial representation of the test conditions is presented in Fig. 4.

For the evaluation, a platoon of four follower vehicles and a leader vehicle was considered. The design considered a standstill spacing, $s_0 = 5$ m and a time-headway, $h = 1$ s.

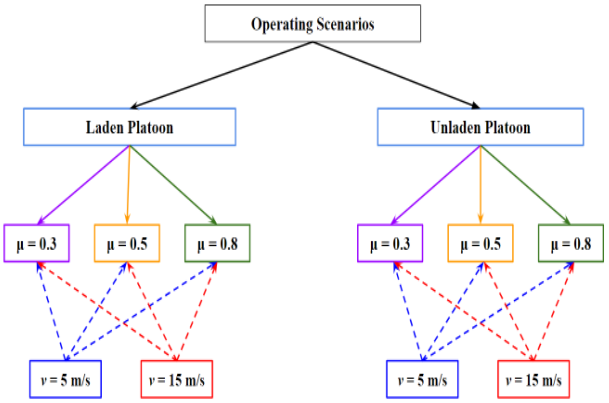

FIGURE 4: Different simulation scenarios.

Other vehicle parameters used in the study are listed in Table 1.

TABLE 1: Vehicle parameters.

Parameter	Value
Wheel radius, r	0.53 m
C.G. height, h_{cg}	1.3 m
Front axle distance from the C.G, l_f	3.4 m
Rear axle distance from the C.G, l_r	2 m
Moment of inertia of front wheels, I_f	10 kgm^2
Moment of inertia of rear wheels, I_r	20 kgm^2

A. IMPORTANCE OF VARIOUS FACTORS CONSIDERED IN THE CONTROLLER DESIGN FRAMEWORK

This subsection discusses the importance of various factors such as vehicle dynamics, actuation dynamics, aerodynamic drag force and lower level controller on the performance of string stable controller design.

1) Importance of Vehicle Dynamics and Actuation Dynamics

To emphasize the importance of considering vehicle dynamics, actuation dynamics and tyre model for designing string stable controllers, results from simulations using kinematic vehicle models are presented in Fig. 5. The string stable controller was designed with the kinematic vehicle model using PRERL based SMC strategy. The position of each vehicle in the platoon on a low-μ (μ=0.3), with a high longitudinal speed (15 m/s) and laden condition, is shown in Fig. 5. It can be observed that in the absence of vehicle dynamics, tyre model, and actuation dynamics, the results show a string stable platoon operation.

Figure 6 represents the scenario of the aforementioned case considering the vehicle dynamics, tyre model and actuator dynamics, in which the platoon ended up in a collision. Here, the string stable controller was designed using PRERL based SMC strategy using the same controller parameters used for kinematic based design. Comparing

This article has been accepted for publication in a future issue of this journal, but has not been fully edited. Content may change prior to final publication. Citation information: DOI 10.1109/ACCESS.2020.3039797, IEEE Access

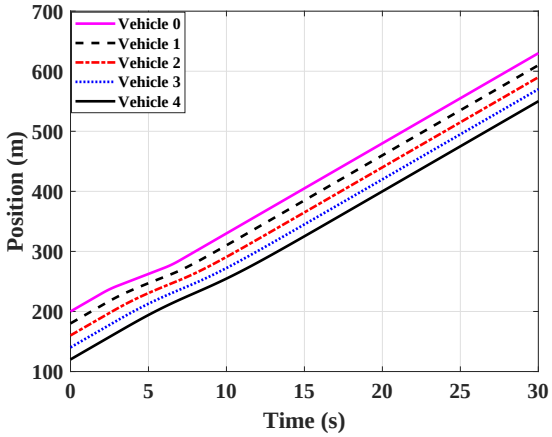

FIGURE 5: Position profile for μ=0.3, high longitudinal speed (15 m/s), laden case without considering vehicle dynamics and actuation dynamics.

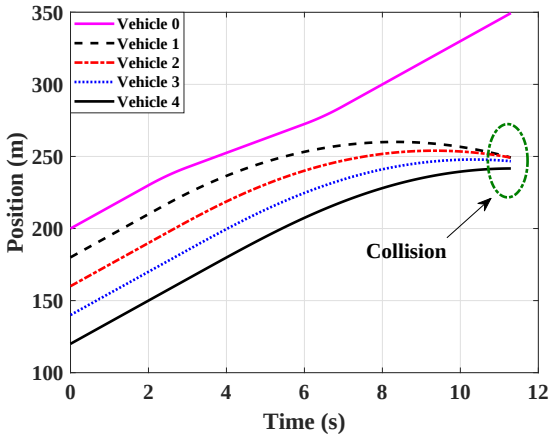

FIGURE 6: Position profile for μ =0.3, high longitudinal speed (15 m/s), laden case, considering vehicle dynamics and actuation dynamics.

Fig. 5 and Fig. 6, one could observe that there lies a discrepancy between the results obtained using kinematic and dynamic models. Since, a dynamic model is better suited to characterise reality in the range of operating conditions considered for platooning, it has been used further.

2) Relevance of Aerodynamic Drag Model

The variation in drag coefficient with respect to intervehicular distance during steady state platoon operation for the case: $\mu = 0.8$, longitudinal speed =15 m/s, laden vehicle, is presented in Fig. 7. For the lead vehicle, the drag coefficient was assumed to be $C_{D0} = 0.8$. A nonlinear drag variation as presented by (6) was used to model the succeeding vehicle drag profiles. For an intermediate vehicle in the platoon, parameter values, $\gamma_1 = 0.2250,\ \gamma_2 = 0.2159, \gamma_3 = 0.1722$, were selected [19]. Figure 8 shows the C_D magnitudes for a vehicle in and not in the platoon formation. From the plot, a clear reduction (≈40%) in the C_D magnitude for the vehicle in platoon formation can be observed. This would in turn reduce the resistive aerodynamic drag force and decrease the torque demand. There was a considerable 35-40% reduction in steady-state demanded torque (per vehicle) compared to the scenario without considering the drag model.

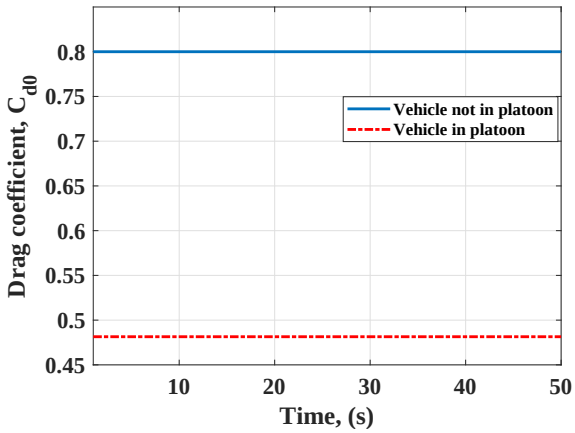

FIGURE 7: Plots of drag coefficient for a laden vehicle with $\mu = 0.8$, and longitudinal speed =15 m/s. $\mu = 0.8$, longitudinal speed =15 m/s, laden vehicle.

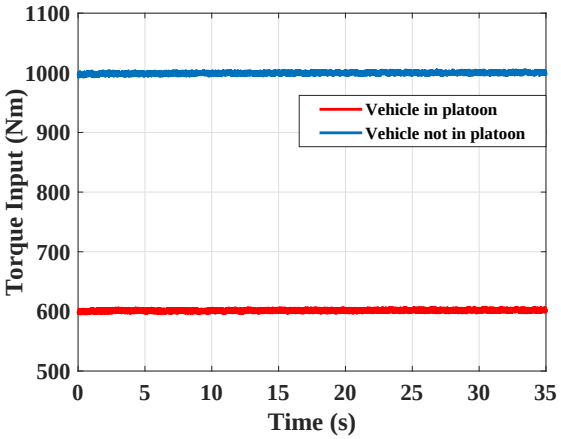

FIGURE 8: Plots of demanded torque for a laden vehicle with $\mu = 0.8$, and longitudinal speed =15 m/s. $\mu = 0.8$, longitudinal speed =15 m/s, laden vehicle.

3) Importance of Lower Level Controller

In order to illustrate the need for a lower level controller in the design framework, string stable controller performance without the incorporation of the designed lower level PID controller has been evaluated. An actuation model with $\tau_d =$ 260 ms and T_d = 45 ms (based on the experimentally corroborated actuation model given in [45] was included for each vehicle in the platoon. It was observed that actuation delay leads to string instability in all the test conditions.

This article has been accepted for publication in a future issue of this journal, but has not been fully edited. Content may change prior to final publication. Citation information: DOI 10.1109/ACCESS.2020.3039797, IEEE Access

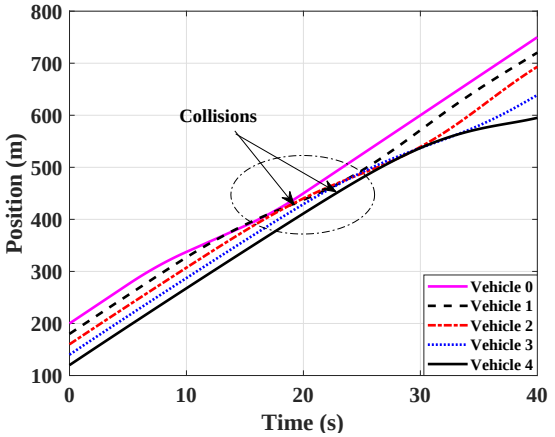

FIGURE 9: Performance without lower level controller ($\mu = 0.8$, longitudinal speed $=15$ m/s, laden vehicle).

Figure 9 shows a sample case ($\mu = 0.8$, longitudinal speed $=15$ m/s, laden vehicle) without lower level controller. Without any delay compensation, the platoon is unable to have a collision-free string-stable operation as presented in Fig. 9. The same scenario was simulated by incorporating the lower level controller and the results are presented in Fig. 10, which shows string stable platoon operation. This shows the significance of lower level controller in the proposed string stable controller design framework.

B. PERFORMANCE EVALUATION IN DIFFERENT OPERATING CONDITIONS

Table 2 shows the various cases used for the evaluation of the proposed string stable controller. The controller parameters for PRERL based SMC were adequately tuned for all the considered test conditions and the best possible controller parameter set, which gave the maximum number of string stable cases, was fixed. The set is given by: $G = 1, \delta_o = 0.1, \alpha = 50, p = 1, \beta = 0.5, \kappa = 0.1, q = 0.9$. The results obtained using the fixed controller parameter set are presented in Table 2.

Results are tabulated for both laden and unladen conditions. A sample result (corresponding to the case, μ=0.8 longitudinal speed=15 m/s, laden case) is shown in Fig. 10. Figure 11 shows the spacing error between consecutive vehicles under the action of the designed string stable controller, for the case: $\mu = 0.8$, longitudinal speed of 15 m/s, and a fully laden vehicle. It can be observed that the spacing error attenuates along the platoon, which shows the efficacy of the string stable controller. From Table 2, it can be observed that the high μ cases resulted in string stable platoon operation, when the general controller parameter set was used. For medium μ cases, using the chosen controller parameter set, all the operating conditions were string stable, except the scenario when the vehicles are laden at high longitudinal speed. Meanwhile, low μ cases resulted in string instability for all the operating conditions when the same controller parameter set was used.

TABLE 2: Performance evaluation under different operating scenarios.

Road Condition (μ)	Longitudinal Speed (m/s)	Load Condition	String Stability (without h adaptation)	String Stability (with h adaptation)
0.8	5	Laden	YES	YES
0.8	5	Unladen	YES	YES
0.8	15	Laden	YES	YES
0.8	15	Unladen	YES	YES
0.5	5	Laden	YES	YES
0.5	5	Unladen	YES	YES
0.5	15	Laden	NO	YES
0.5	15	Unladen	YES	YES
0.3	5	Laden	NO	YES
0.3	5	Unladen	NO	YES
0.3	15	Laden	NO	YES
0.3	15	Unladen	NO	YES

This shows that the type of road surface has a significant effect on platoon stability and hence controller design incorporating vehicle dynamics and tyre model is extremely important for string stable platooning. This also emphasizes the need for an adaptive string stability controller, that can tune the controller parameters with respect to the road surfaces. However, realization of such a controller requires online information on road surface, which is practically not tractable. To tackle this issue, a method to adaptively vary the time-headway in the controller design framework such that string stability is guaranteed at varying speed and road conditions is presented next.

C. ADAPTIVE TIME-HEADWAY BASED STRING STABLE CONTROLLER

The string stable controller has been designed such that the desired inter-vehicular distance (s_d) between two vehicles in the platoon is governed by the expression given in (16). In this expression the time-headway, h_i was considered as constant. From the studies presented above (Table 2), it was found that in certain road conditions, the vehicle was not be able to realize the brake/traction force demanded by the string stable controller and the spacing error propagates along the platoon, leading to string instability. To address this issue, the time-headway is modified by the following adaptive equation that drives spacing error to zero at each instant:

$$h_i(t) = \frac{x_{i-1}(t) - x_i(t) - s_o}{v_i(t)}. \tag{62}$$

This adaptive equation is derived such that the spacing error defined by (17) is driven to zero at each instant. However, this can not be true always. Factors such as actuator dynamics and communication delays have not been considered for calculating $e_i(t)$ in the formulation. However, in practice, this error would be influenced by these factors. Hence, there would be discrepancies between the actual

This article has been accepted for publication in a future issue of this journal, but has not been fully edited. Content may change prior to final publication. Citation information: DOI 10.1109/ACCESS.2020.3039797, IEEE Access

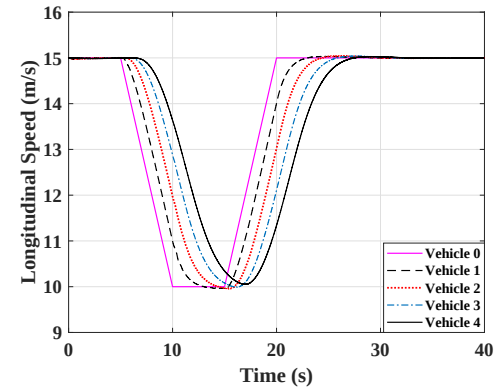

(a) Longitudinal speed vs. Time.

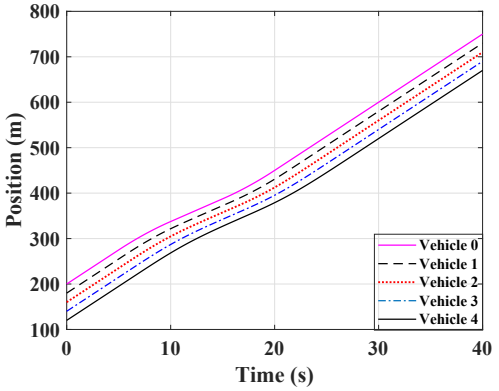

(b) Position vs. Time.

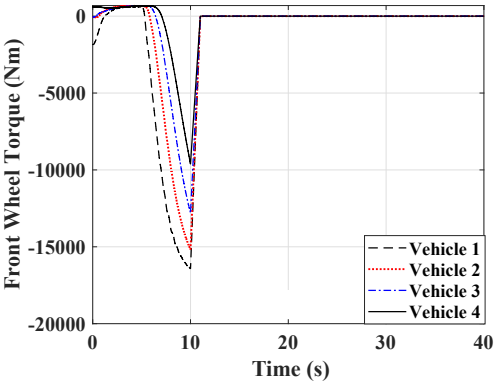

(c) Front wheel torque input vs. Time.

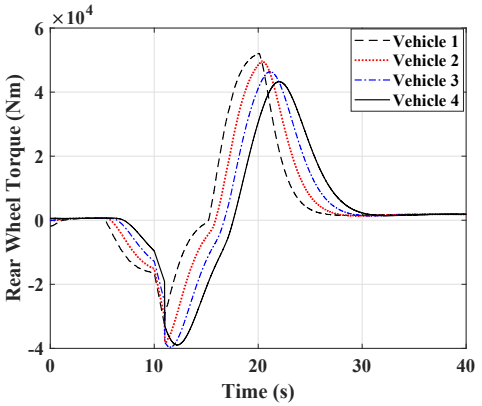

(d) Rear wheel torque input vs. Time.

FIGURE 10: μ =0.8, longitudinal speed = 15 m/s, laden case: for torque input plots, positive value indicates drive torque and negative value indicates braking torque.

spacing error (from the vehicle model incorporating actuator dynamics and communication delays) and the ideal spacing error (defined by (17)). As a result, the actual error always takes a non-zero value, even if one tries to make it to zero through time-headway adaptation. Hence, it is important to consider this actual spacing error throughout the perturbation maneuver and to attenuate it through instantaneous time-headway adaptation.

The designed sliding mode control based string stable controller uses the instantaneous values of $h_i(t)$ (according to (62)) and tries to bring the actual intervehicular distance $d_i(t)$ to the desired distance $s_d(t)$ at each instant of time. In the desired inter-vehicular distance expression $s_d(t) = s_o + h_i(t)v_i(t)$, s_o is a constant and indicates stand-still spacing (that is, the spacing between two consecutive vehicles when all the vehicles in the platoon are at rest). So, one could essentially consider s_o as the minimum value of $s_d(t)$, and hence $d_i(t)$. The controller always tries to maintain this minimum intervehicular distance between the vehicles, equal to the stand-still spacing value, even in the worst case scenarios to maintain a string stable operation. This is valid even when $v_i(t) = 0$, when the platoon stops

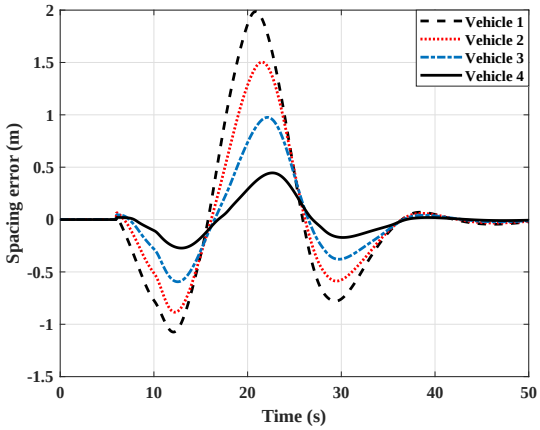

FIGURE 11: Plots showing the spacing error attenuation (μ = 0.8, longitudinal speed =15 m/s, laden vehicle - constant time-headway policy).

This article has been accepted for publication in a future issue of this journal, but has not been fully edited. Content may change prior to final publication. Citation information: DOI 10.1109/ACCESS.2020.3039797, IEEE Access

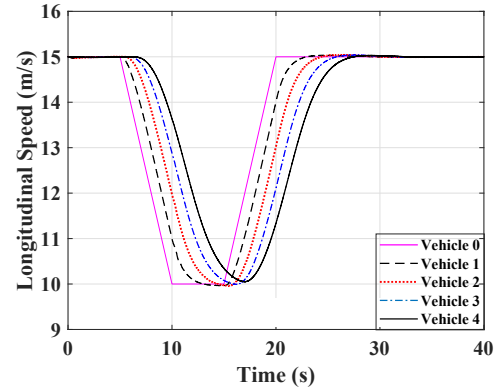

(a) Longitudinal speed vs. Time.

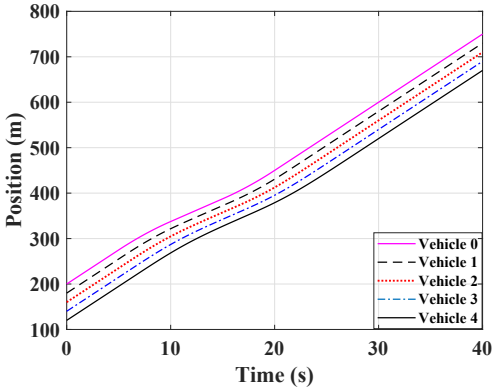

(b) Position vs. Time.

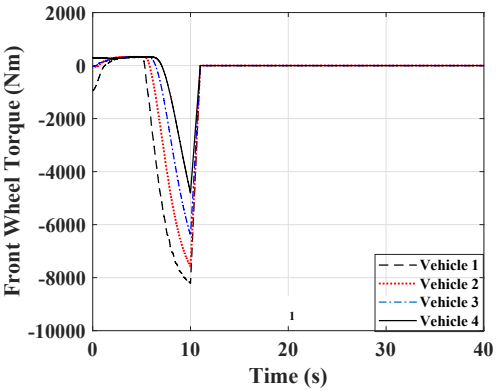

(c) Front wheel torque input vs. Time.

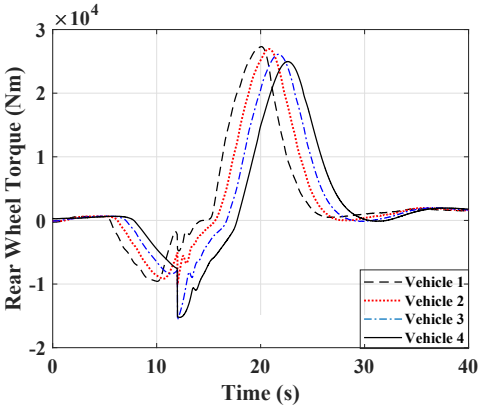

(d) Rear wheel torque input vs. Time.

FIGURE 12: Adaptive time-headway policy-μ=0.3, longitudinal speed = 15 m/s, laden case: for torque input plots, (positive value indicates drive torque and negative value indicates braking torque).

(since s_o can be ideally interpreted as the distance between 2 consecutive vehicles when the vehicles come to rest). This means that the value of $d_i(t)$ would never decrease to 0, since $s_o \neq 0$.

It is to be noted that for the synthesis of adaptive time-headway at each instant, the current positions of the preceding vehicle and the host vehicle, and the longitudinal speed of the host vehicle are required. These information are already been assumed to be available for the constant time-headway policy. Hence, the practical implementation of the adaptive time-headway strategy does not add additional data requirement.

1) Performance Evaluation of Adaptive Time-Headway Based Design

All the operating scenarios considered in Table 2 were evaluated for string stability using the proposed adaptive time-headway based PRERL controller. These results are also tabulated in Table 2. It can be observed that string stability has been achieved in all the operating scenarios irrespective of the road conditions, when the general controller parameter set was used along with time-headway adaptation. A sample result, corresponding to the case, μ =0.3, longitudinal speed=15 m/s, laden case (one of the

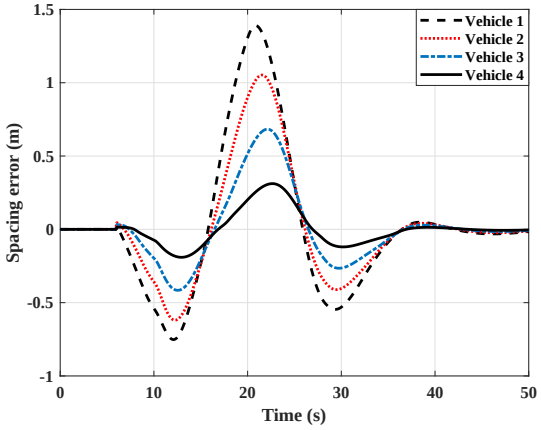

FIGURE 13: Plots showing the spacing error attenuation (μ = 0.3, longitudinal speed =15 m/s, laden vehicle - adaptive time-headway policy).

This article has been accepted for publication in a future issue of this journal, but has not been fully edited. Content may change prior to final publication. Citation information: DOI 10.1109/ACCESS.2020.3039797, IEEE Access

cases, which resulted in string instability using the constant time-headway approach), is shown in Fig. 12. Figure 13 shows the efficacy of the proposed adaptive time-headway-based string stable controller in attenuating the spacing error between the vehicles along the platoon.

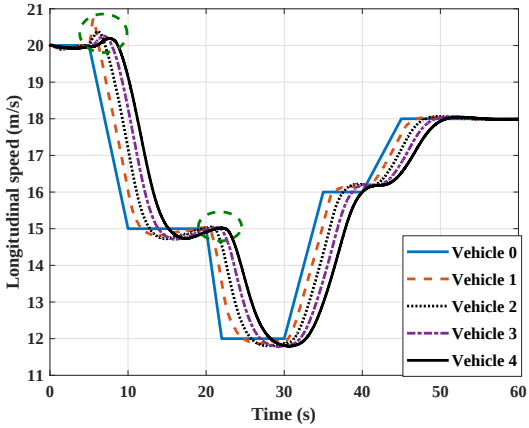

FIGURE 14: Longitudinal speed profile tracking for a varying speed perturbation signal

Also, the efficacy of the proposed time-headway adaptation policy has been tested for other speed perturbation signals of different magnitudes, frequencies and profiles, and found that string stability was always ensured with h adaptation for these signals. The longitudinal speed tracking profile for another speed perturbation signal (represented by v_0) is shown in Fig. 14. The sample result shown in Fig. 14 corresponds to the case with $\mu = 0.8$ and fully laden condition. It was observed that string stability was ensured with h adaptation for all test conditions presented in Table 2, even with this speed perturbation signal.

In this paper, the first order Padé approximation has been used to obtain a finite order transfer function to represent the actuator model, which incorporates the effects of actuation (brake) system time delay. Time delay compensation via the first order Padé approximation would make the system non-minimum phase, due to the introduction of a zero in the right half complex plane. The impact of the non-minimum phase zero introduced due to the Padé approximation can be observed (initially the response is in the opposite direction of the intended tracking profile) from the circled portions in the longitudinal speed curves in Fig. 14.

2) Adaptive Time-Headway Policy - Dynamic Analysis

During a longitudinal speed perturbation maneuver, let the actual spacing error be given by,

$$e_{i_p}(t) = d_{i_p}(t) - s_{d_p}(t), \tag{63}$$

where, $d_{i_p}(t)$ represents the actual spacing between two vehicles and $s_{d_p}(t)$ represents the desired inter-vehicular distance in presence of a longitudinal speed perturbation. Now, considering the discrepancy between the actual spacing error and the ideal spacing error, the equation characterising the variation of time-headway (h) under the influence of a longitudinal speed perturbation can be written as

$$h_{i_p}(t) = \frac{d_{i_p}(t) - s_o}{v_{i_p}(t)}. \tag{64}$$

In (64), $v_{i_p}(t)$ represents the longitudinal speed perturbation and $h_{i_p}(t)$ represents the time-headway variations.

Now, during the perturbation maneuver, $d_{i_p}(t) = x_{i-1_p}(t) - x_{i_p}(t)$, where $x_{i-1_p}(t)$ and $x_{i_p}(t)$ represent the positions of two consecutive vehicles during the speed perturbation. Hence, equation (64) can be written as,

$$h_{i_p}(t) = \frac{x_{i-1_p}(t) - x_{i_p}(t) - s_o}{v_{i_p}(t)}. \tag{65}$$

This expression represents the adaptive time-headway variation in terms of the actual error values during any perturbation maneuver. Now, taking the time derivative of the above equation,

$$\dot{h}_{i_p}(t) = \frac{v_{i_p}(t)(v_{i-1_p}(t) - v_{i_p}(t)) - (x_{i-1_p}(t) - x_{i_p}(t) - s_o)}{v_{i_p}^2(t)}. \tag{66}$$

For constant time-headway policy, time-headway, $h_{i_p}(t) = h$ is constant and its time derivative is zero. Then,

$$\frac{v_{i_p}(t)(v_{i-1_p}(t) - v_{i_p}(t)) - (x_{i-1_p}(t) - x_{i_p}(t) - s_o)}{v_{i_p}^2(t)} = 0. \tag{67}$$

From equation (67), one can solve for $v_{i_p}(t)$ and on substituting the condition for collision-free operation, i. e., $d_{i_p}(t) = s_o + hv_{i_p}(t)$,

$$v_{i_p}(t) = \frac{v_{i-1_p}(t) \pm \sqrt{v_{i-1_p}^2(t) - 4ha_{i_p}(t)}}{2}, \tag{68}$$

from which, the restriction on the achievable acceleration/deceleration $a_{i_p}(t)$ during the perturbation maneuver can be presented as, be presented as,

$$a_{i_p}(t) = \frac{v_{i-1_p}(t) - v_{i_p}(t)}{h}. \tag{69}$$

For constant time-headway policy, the maximum value of acceleration/deceleration is limited by the value of h, which is considered to be constant throughout the operation. This limits the capability of the policy in achieving acceleration/deceleration magnitudes that could be required for having a string stable operation for certain road conditions as presented in Table 2.

In this paper, an attempt is made to solve this problem by proposing the so-called adaptive time-headway policy, where $h_{i_p}(t)$ is modelled as a time varying quantity. Hence, the derivative of $h_{i_p}(t)$ exists and from (66), and on using

This article has been accepted for publication in a future issue of this journal, but has not been fully edited. Content may change prior to final publication. Citation information: DOI 10.1109/ACCESS.2020.3039797, IEEE Access

the condition for collision-free operation, i. e., $d_{i_p}(t) = s_o + hv_{i_p}(t)$, $a_{i_p}(t)$ can be obtained as,

$$a_{i_p}(t) = \frac{v_{i-1_p}(t) - v_{i_p}(t)(1 + \dot{h}_{i_p}(t))}{h_{i_p}(t)}. \tag{70}$$

In this policy, $a(t)$ is allowed to vary as a function of $h(t)$ as presented by equation (62). Both $h(t)$ and its derivative dynamics affect the maximum achievable acceleration/deceleration limit. The higher levels of acceleration/deceleration demand while using the constant time-headway policy for unstable scenarios was reduced within reasonable limits using the adaptive time-headway policy. This resulted in string stable operation in the previously unstable scenarios as presented in Table 2.

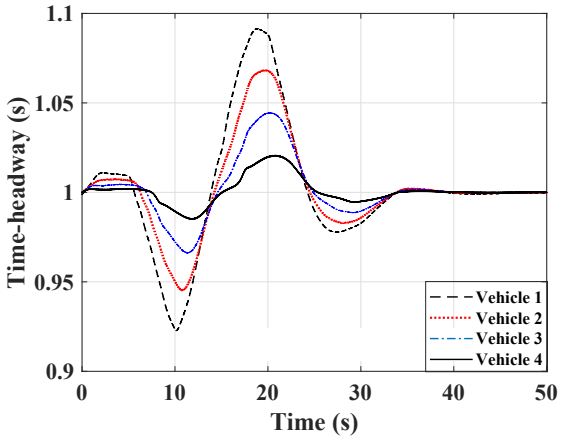

FIGURE 15: Temporal variation of h: μ=0.8, longitudinal speed=15 m/s, laden case.

3) Effect of Time-headway Adaptation on Aerodynamic Drag Force

Now, an argument can be made with respect to the selection of intervehicular distance for a platoon operating at different scenarios. If one chooses to design a platoon with sufficiently large intervehicular distance, string stability would be achieved even for low μ operating conditions. However, this would be at the cost of increased aerodynamic drag (since aerodynamic drag is a function of intervehicular distance) and consequently reduced fuel economy, thus undermining the crucial advantage of platoon operation. Hence, it is imperative to choose the intervehicular distance value as small as possible in order to have an efficient platoon operation. This concern is also addressed during the adaptive time-headway operation. Figure 15 presents the adaptive variation of time-headway for a platoon operating at 15 m/s on a high-μ (0.8) road. In the constant time-headway counter part, the time-headway magnitude was kept constant ($h = 1$ s) throughout the entire operation. Corresponding to the h variations as presented in Fig. 15, intervehicular distances also vary according to $d_i(t) = s_o + h_i(t)v_i(t)$. In the constant time-headway approach this variation was governed

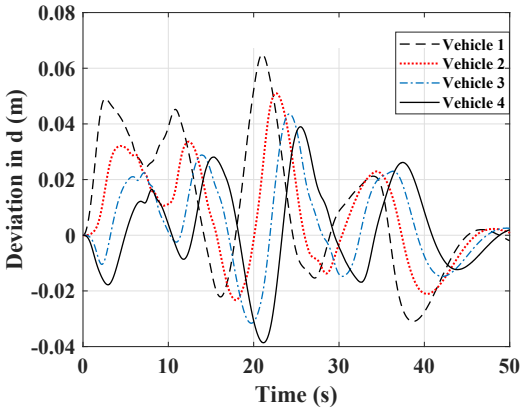

(a) Longitudinal speed vs. Time.

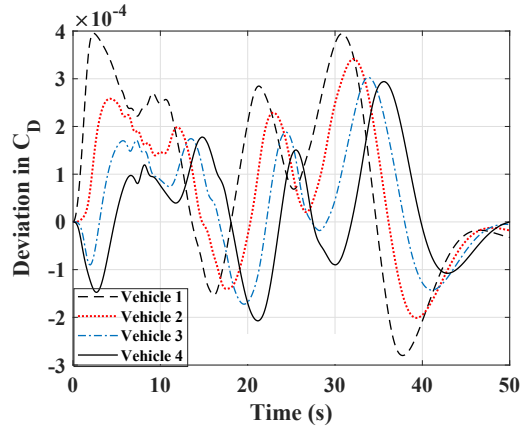

(b) Position vs. Time.

FIGURE 16: Plots of difference in intervehicular distance and drag coefficient with and without h adaptation for a laden vehicle with $\mu = 0.8$, and longitudinal speed =15 m/s.

by (16). A plot showing the variation in intervehicular distance with time-headway adaptation and without adaptation is presented in Fig. 16(a). As observed, the difference in intervehicular distance between each vehicle in platoon is small, but enough for a stable platoon operation. Similarly, the difference in drag coefficient (C_D) magnitude is also presented in Fig. 16(b). The deviation in C_D is in the order of 10^{-4}. When compared to the magnitude of C_{D0} (0.8), this deviation in C_D is insignificant, thus indicating a string stable platoon operation without significant increase in torque demand (similar observations were made for all the considered operating conditions given in Table 2).

D. EFFECT OF COMMUNICATION DELAY ON STRING STABILITY

In the presented design framework, information from the preceding vehicle is required to synthesise control action for platoon string stability and this information can be obtained through RADAR. However, the platoon may encounter sce-

This article has been accepted for publication in a future issue of this journal, but has not been fully edited. Content may change prior to final publication. Citation information: DOI 10.1109/ACCESS.2020.3039797, IEEE Access

narios where the RADAR may not function well. RADAR sensor measurements are affected by signal attenuation by the medium, beam dispersion, noises, interference, multi-object echo, and jamming [50]. A platoon cannot tolerate such a scenario, since the malfunctioning of the RADAR system in one vehicle can lead to string instability of the entire platoon. In such scenarios, V2V communication-based data transfer facility in vehicles becomes important. If V2V communication option is provided as a back-up method for data transfer, one can rely on it for obtaining velocity and position information in scenarios when RADAR information is not readily available. Moreover, telematics systems that exchange information between vehicles during fleet operation are made mandatory in heavy vehicles in countries like India [51]. This would help to switch to V2V communication-based data transmission in future. Motivated by these aspects, the notion of platoon string stability from a connected vehicle technology perspective has also been investigated. Since, this paper mainly deals with various extreme operating scenarios during HCRV platooning, the communication delay involved in V2V communication has also been analysed.

The string stable controller performance has been analysed by considering constant time-headway as well as adaptive time-headway design approaches. It was assumed that a fixed communication delay is present during data transmission from the preceding vehicle and simulations were run to obtain the maximum delay magnitude, which could guarantee string stability. The control equations for string stability (given by (27) and (28)) were influenced by this assumption. Hence, the control equations were modified as follows:

$$\tau_i(t) = \frac{-1}{qh_i\Lambda}\Bigg[\frac{-G}{\delta_0+(1-\delta_0)e^{-\alpha|S_i(t)|^p}}|S_i(t)|^\beta \mathrm{sign}(S_i(t)) - q(v_{i-1}(t-\tau_c)-v_i(t)) - q\kappa e_i(t) + \dot{e}_{i+1}(t) + \kappa e_{i+1}(t) + qh_i\Gamma\Bigg], \quad i=1,...,N-1, \tag{71}$$

$$\tau_N(t) = \frac{-1}{qh_N\Lambda}\Bigg[\frac{-G}{\delta_0+(1-\delta_0)e^{-\alpha|S_N(t)|^p}}|S_N(t)|^\beta \mathrm{sign}(S_N(t)) - q(v_{N-1}(t-\tau_c)-v_N(t)) - q\kappa e_i(t) + qh_N\Gamma\Bigg]. \tag{72}$$

Here, τ_c represents the fixed communication latency magnitude. Table 3 shows the observations on the delay limits for different operating conditions. As given in Table 2, some cases are string unstable even without the incorporation of communication delay, while constant time-headway approach was used. Delay tolerance corresponding to these cases are indicated by '-' in Table 3.

From Table 3, it can be observed that compared to constant time-headway approach, the adaptive time-headway based controller design is more tolerant to communication delay. However, the string stability which was established using adaptive time-headway policy has been lost with the incorporation of communication delay on low μ road surfaces, when the longitudinal speed of the vehicle is high. This could be attributed to the brake/drive dynamics of the HCRV under low μ road conditions. From a practical point of view, a vehicle plying on a low μ road needs more time to safely accelerate/decelerate to a new speed owing to the reduced traction at tyre-road interface (for instance, the stopping distance on a low μ surface would be much higher compared to high and medium μ roads). Presence of further delays during the operation, in form of communication delay, aggravates this condition. The communication latency further delays the computation of control signals to be applied to throttle and brake actuators. On a low μ surface, this delay could be more than what the controller can handle to effectively have an autonomous string stable platoon operation. However, at low operating speed (5 m/s), the adaptive time-headway policy manages to tolerate communication delay of reasonable magnitudes (40 ms for laden scenario and 140 ms for unladen scenario).

TABLE 3: Communication delay limits.

Road Condition μ	Longitudinal Speed (m/s)	Load Condition	Maximum Communication Delay Magnitude (ms)	
			Constant h	With h adaptation
0.8	5	Laden	560	920
0.8	5	Unladen	580	960
0.8	15	Laden	200	520
0.8	15	Unladen	220	630
0.5	5	Laden	320	780
0.5	5	Unladen	340	830
0.5	15	Laden	-	270
0.5	15	Unladen	60	300
0.3	5	Laden	-	40
0.3	5	Unladen	-	140
0.3	15	Laden	-	0
0.3	15	Unladen	-	0

V. CONCLUSION

This paper attempts an approach for the design and analysis of heavy vehicle platoons and their stability to ensure collision-free operation under various operating conditions. The majority of literature on string stable platoon design have considered kinematics alone, or opting for only some of the considered dynamic factors. But to emulate the real life conditions like a sudden change in road conditions, it is imperative to consider the corresponding scenarios in the analysis. Further, there is a significant difference in the laden and unladen mass of HCRVs (the laden mass is 16200 kg and the unladen mass is 4700 kg for the class of vehicles considered in this study) that would impact the vehicle dynamic response, and this has been considered in this study. In this regard, a platoon model incorporating detailed vehicle dynamics, with wheel dynamics, resistive forces, tyre model, actuation dynamics and communication delays has been presented in this paper. The major contributions of the paper are:

1) A Sliding Mode Control (SMC) based string stable controller has been designed and evaluated through simulating platoon operation for different on-road conditions. In order to have an actuator friendly controller design, SMC approach based on Power Rate Exponential Reaching Law (PRERL) has been used, which was seen to ensure feasible traction/brake inputs for string stable platoon operation. A lower level PID controller that could increase the fidelity of the string stable controller has also been been designed.
2) To ensure string stable operation on various on-road conditions, an adaptive time-headway based method has been introduced in the string stable controller design framework. It was observed that, as long as the adaptive policy is used, the platoon is more tolerant to V2V communication delay.

The adaptive string stable controller design strategy presented in this paper can be suitably utilized for realizing string stable heavy vehicle platoon during long haul operations, where the road conditions would vary considerably due to various environmental factors. However, on low μ road surfaces, the proposed controller design could not handle significant communication delays. Addressing this issue could be pursued as part of future work.

The string stable controller has been currently designed based on the assumption that the heavy vehicle platoon travels on a straight and flat road. Also, the tyre model parameters and vehicle parameters were assumed to be known. These assumptions would be relaxed with appropriate road gradient estimation, μ estimation and vehicle mass estimation schemes while pursuing further extension and real-time implementation of the presented work.

APPENDIX. STATE SPACE REPRESENTATION OF THE COMPLETE SYSTEM DYNAMICS MODEL

The state space representation of the position and speed dynamics can be represented as:

$$\begin{aligned} \dot{x}_i(t) &= v_i(t) \\ \dot{v}_i(t) &= \Omega(v_i(t), \tau_i(t)), \end{aligned} \tag{73}$$

where, $\Omega(v_i(t), \tau_i(t))$ is a nonlinear function in $v_i(t)$ and $\tau_i(t)$ that can be expressed as

$$\Omega(v_i(t), \tau_i(t)) = \frac{1}{m_i}(F_{xfi}(\lambda_{fi}(t)) + F_{xri}(\lambda_{ri}(t)) - F_{Ri}(t)), \tag{74}$$

where, $F_{xfi}(\lambda_{fi}(t))$ and $F_{xri}(\lambda_{ri}(t))$ represent the longitudinal forces at the front and rear tyre-road interface respectively, and $\lambda_{fi}(t)$ and $\lambda_{ri}(t)$ represent the longitudinal slip ratios of front and rear wheels respectively. They are calculated as,

$$\begin{aligned} \lambda_{fi}(t) &= \frac{v_i(t) - r_i\ \omega_{fi}(t)}{v_i(t)}, \\ \lambda_{ri}(t) &= \frac{v_i(t) - r_i\ \omega_{ri}(t)}{v_i(t)}, \end{aligned} \tag{75}$$

where, r_i is the tyre radius. From the wheel dynamics, ω_{fi} and ω_{ri} can be calculated as,

$$\begin{aligned} \dot{\omega}_{fi}(t) &= \frac{1}{I_{fi}}(\tau_{fi}(t) - r_i F_{xfi}(t)), \\ \dot{\omega}_{ri}(t) &= \frac{1}{I_{ri}}(\tau_{ri}(t) - r_i F_{xri}(t)), \end{aligned} \tag{76}$$

where, I_{fi} and I_{ri} are the moment of inertia of front and rear wheels respectively, $\tau_{fi}(t)$ and $\tau_{ri}(t)$ are the transmitted torques to the front and rear wheels respectively.

Now, $F_{Ri}(t)$ in (74) can be expressed as,

$$\begin{aligned} F_{Ri}(t) &= F_{ai}(t) + R_{xfi}(t) + R_{xri}(t) \\ &= \rho\ a_{fi}\ C_{Di}(t)\frac{v_i(t)^2}{2} + f(F_{zfi}(t) + F_{zri}(t)), \end{aligned} \tag{77}$$

where, $F_{ai}(t)$ represents the force due to aerodynamic drag, and R_{xfi} and R_{xri} are the forces due to rolling resistance at the front and rear wheels respectively. The aerodynamic drag force is characterised by the air density, ρ, the aerodynamic drag coefficient, $C_{Di}(t)$, and the vehicle frontal area, a_{fi}. The rolling resistance is characterised by the rolling resistance coefficient, f, and the normal forces on both front and rear tyres, represented respectively by $F_{zfi}(t)$ and $F_{zri}(t)$. The normal forces at the tyre-road interface are given by,

$$\begin{aligned} F_{zfi}(t) &= \frac{mgl_r - F_{ai}(t)\ h_a - ma_i(t)h_{cg}}{l_f + l_r}, \\ F_{zri}(t) &= \frac{mgl_f + F_{ai}(t)\ h_a + ma_i(t)h_{cg}}{l_f + l_r}, \end{aligned} \tag{78}$$

where, $a_i(t)$ is the longitudinal acceleration, h_{cg} is the height of the C.G. of the vehicle, h_a is the height of the location at which the equivalent aerodynamic force acts, and l_f and l_r are the longitudinal distance of the front axle and rear axle from the C.G. of the vehicle.

The transfer function of the actuator dynamics is given by

$$P(s) = \frac{\tau_i(s)}{\tau_{des}(s)} = \frac{1}{1 + \tau_d s}e^{-T_d s}, \tag{79}$$

where, τ_d is the time constant, and T_d is the time delay, and τ_{des} and τ_i represent the demanded brake torque and actual brake torque developed, respectively.

Using first order Padé approximation, the actuation model (79) can be rewritten as

$$P(s) \approx \frac{(2 - T_d s)}{(1 + s\tau_d)(2 + T_d s)}. \tag{80}$$

Considering the brake torque dynamics in the front wheels of the i^{th} vehicle, the state space equation of (80) can be written as

$$\begin{bmatrix} \dot{\tau}_{1fi}(t) \\ \dot{\tau}_{2fi}(t) \end{bmatrix} = \begin{bmatrix} 0 & 1 \\ \frac{-2}{\tau_d T_d} & -(\frac{1}{\tau_d} + \frac{2}{T_d}) \end{bmatrix} \begin{bmatrix} \tau_{1fi}(t) \\ \tau_{2fi}(t) \end{bmatrix} + \begin{bmatrix} 0 \\ 1 \end{bmatrix} \tau_{desfi}(t), \tag{81}$$

$$\tau_{fi}(t) = \begin{bmatrix} \frac{2}{T_d\tau_d} \\ \\ \frac{-1}{\tau_d} \end{bmatrix} \cdot \begin{bmatrix} \tau_{1fi}(t) \\ \tau_{2fi}(t) \end{bmatrix}, \tag{82}$$

and the brake torque dynamics in the rear wheels of the i^{th} vehicle can be written as

$$\begin{bmatrix} \dot{\tau}_{1ri}(t) \\ \dot{\tau}_{2ri}(t) \end{bmatrix} = \begin{bmatrix} 0 & 1 \\ \frac{-2}{\tau_d T_d} & -(\frac{1}{\tau_d} + \frac{2}{T_d}) \end{bmatrix} \begin{bmatrix} \tau_{1ri}(t) \\ \tau_{2ri}(t) \end{bmatrix} + \begin{bmatrix} 0 \\ 1 \end{bmatrix} \tau_{desri}(t), \tag{83}$$

$$\tau_{ri}(t) = \begin{bmatrix} \frac{2}{T_d\tau_d} \\ \\ \frac{-1}{\tau_d} \end{bmatrix} \cdot \begin{bmatrix} \tau_{1ri}(t) \\ \tau_{2ri}(t) \end{bmatrix}. \tag{84}$$

Now, on substituting $\tau_{1fi}(t)$, $\tau_{2fi}(t)$ from (82) and (84) in (76), the wheel dynamics can be expressed as

$$\begin{aligned} \dot{\omega}_{fi}(t) &= \frac{1}{I_{fi}}\Big(\frac{2}{T_d\tau_d}\tau_{1fi}(t) - \frac{1}{\tau_d}\tau_{2fi}(t) - r_i F_{xfi}(t)\Big), \\ \dot{\omega}_{ri}(t) &= \frac{1}{I_{ri}}\Big(\frac{2}{T_d\tau_d}\tau_{1ri}(t) - \frac{1}{\tau_d}\tau_{2ri}(t) - r_i F_{xri}(t)\Big). \end{aligned} \tag{85}$$

Considering the above discussed complete vehicle model including actuator dynamics, the entire state space representation for a single vehicle in the platoon can be represented in the following state vector form:

$$\dot{\boldsymbol{\phi}}_i(t) = \mathbf{f}(\boldsymbol{\phi}_i(t), \mathbf{u}_i(t)), \tag{86}$$

where, the state vector $\boldsymbol{\phi}_i(t) = \big[x_i(t)\ v_i(t)\ \omega_{fi}(t)\ \omega_{ri}(t)\ \tau_{1fi}(t)\ \tau_{2fi}(t)\ \tau_{1ri}(t)\ \tau_{2ri}(t)\big]^T$, and the input vector $\mathbf{u}_i(t) = \big[\tau_{desfi}(t)\ \tau_{desri}(t)\big]^T$.

CONFLICT OF INTEREST

The authors declare no potential conflicts of interest with respect to the research, authorship, and/or publication of this article.

ACKNOWLEDGEMENTS

The authors thank the Ministry of Skill Development and Entrepreneurship, Government of India, for funding through the grant EDD/14-15/023/MOLE/NILE.

REFERENCES

[1] S. W. Smith, Y. Kim, J. Guanetti, R. Li, R. Firoozi, B. Wootton, A. A. Kurzhanskiy, F. Borrelli, R. Horowitz, and M. Arcak, "Improving urban traffic throughput with vehicle platooning: Theory and experiments," IEEE Access, vol. 8, pp. 141 208–141 223, 2020.

[2] C. Zhai, X. Chen, C. Yan, Y. Liu, and H. Li, "Ecological cooperative adaptive cruise control for a heterogeneous platoon of heavy-duty vehicles with time delays," IEEE Access, vol. 8, pp. 146 208–146 219, 2020.

[3] K. Yu, Q. Liang, J. Yang, and Y. Guo, "Model predictive control for hybrid electric vehicle platooning using route information," Proceedings of the Institution of Mechanical Engineers, Part D: Journal of Automobile Engineering, vol. 230, no. 9, pp. 1273–1285, 2016.

[4] K. Yu, H. Yang, X. Tan, T. Kawabe, Y. Guo, Q. Liang, Z. Fu, and Z. Zheng, "Model predictive control for hybrid electric vehicle platooning using slope information," IEEE Transactions on Intelligent Transportation Systems, vol. 17, no. 7, pp. 1894–1909, 2016.

[5] D. Swaroop, J. K. Hedrick, C. Chien, and P. Ioannou, "A comparision of spacing and headway control laws for automatically controlled vehicles," Vehicle System Dynamics, vol. 23, no. 1, pp. 597–625, 1994.

[6] D. Swaroop, "String stability of interconnected systems: An application to platooning in automated highway systems," 1997.

[7] J. Ploeg, N. Van De Wouw, and H. Nijmeijer, "Lp string stability of cascaded systems: Application to vehicle platooning," IEEE Transactions on Control Systems Technology, vol. 22, no. 2, pp. 786–793, 2013.

[8] J.-W. Kwon and D. Chwa, "Adaptive bidirectional platoon control using a coupled sliding mode control method," IEEE Transactions on Intelligent Transportation Systems, vol. 15, no. 5, pp. 2040–2048, 2014.

[9] Y. Zheng, S. E. Li, J. Wang, D. Cao, and K. Li, "Stability and scalability of homogeneous vehicular platoon: Study on the influence of information flow topologies," IEEE Transactions on Intelligent Transportation Systems, vol. 17, no. 1, pp. 14–26, 2015.

[10] X. Guo, J. Wang, F. Liao, and R. S. H. Teo, "Distributed adaptive integrated-sliding-mode controller synthesis for string stability of vehicle platoons," IEEE Transactions on Intelligent Transportation Systems, vol. 17, no. 9, pp. 2419–2429, 2016.

[11] K. B. Devika, N. Sridhar, V. R. S. Yellapantula, and S. C. Subramanian, "Control of heavy road vehicle platoons incorporating actuation dynamics," in TENCON 2019-2019 IEEE Region 10 Conference (TENCON). IEEE, 2019, pp. 1434–1439.

[12] Y. Li, C. Tang, S. Peeta, and Y. Wang, "Integral-sliding-mode braking control for a connected vehicle platoon: Theory and application," IEEE Transactions on Industrial Electronics, vol. 66, no. 6, pp. 4618–4628, 2018.

[13] G. Gunter, C. Janssen, W. Barbour, R. Stern, and D. Work, "Model based string stability of adaptive cruise control systems using field data," IEEE Transactions on Intelligent Vehicles, vol. 5, no. 1, pp. 90–99, 2019.

[14] J. Wang, X. Luo, L. Wang, Z. Zuo, and X. Guan, "Integral sliding mode control using a disturbance observer for vehicle platoons," IEEE Transactions on Industrial Electronics, vol. 67, no. 8, pp. 6639–6648, 2019.

[15] S. Feng, Y. Zhang, S. E. Li, Z. Cao, H. X. Liu, and L. Li, "String stability for vehicular platoon control: Definitions and analysis methods," Annual Reviews in Control, vol. 47, pp. 81–97, 2019.

[16] J. Ploeg, E. Semsar-Kazerooni, G. Lijster, N. van de Wouw, and H. Nijmeijer, "Graceful degradation of cooperative adaptive cruise control," IEEE Transactions on Intelligent Transportation Systems, vol. 16, no. 1, pp. 488–497, 2014.

[17] S. Baldi, D. Liu, V. Jain, and W. Yu, "Establishing platoons of bidirectional cooperative vehicles with engine limits and uncertain dynamics," IEEE Transactions on Intelligent Transportation Systems, 2020.

[18] C. Zhai, Y. Liu, and F. Luo, "A switched control strategy of heterogeneous vehicle platoon for multiple objectives with state constraints," IEEE Transactions on Intelligent Transportation Systems, vol. 20, no. 5, pp. 1883–1896, 2018.

[19] A. A. Hussein and H. A. Rakha, "Vehicle platooning impact on drag coefficients and energy/fuel saving implications," arXiv preprint arXiv:2001.00560, 2020.

[20] C. Zhai, F. Luo, Y. Liu, and Z. Chen, "Ecological cooperative look-ahead control for automated vehicles travelling on freeways with varying slopes," IEEE Transactions on Vehicular Technology, vol. 68, no. 2, pp. 1208–1221, 2018.

[21] C. Zhai, F. Luo, and Y. Liu, "Cooperative look-ahead control of vehicle platoon for maximizing fuel efficiency under system constraints," IEEE Access, vol. 6, pp. 37 700–37 714, 2018.

[22] S. Gong, J. Shen, and L. Du, "Constrained optimization and distributed computation based car following control of a connected and autonomous vehicle platoon," Transportation Research Part B: Methodological, vol. 94, pp. 314–334, 2016.

[23] D. Swaroop, J. K. Hedrick, and S. B. Choi, "Direct adaptive longitudinal control of vehicle platoons," IEEE Transactions on Vehicular Technology, vol. 50, no. 1, pp. 150–161, 2001.

[24] A. Rupp, M. Steinberger, and M. Horn, "Sliding mode based platooning with non-zero initial spacing errors," IEEE Control Systems Letters, vol. 1, no. 2, pp. 274–279, 2017.

[25] V. Utkin, "Variable structure systems with sliding modes," IEEE Transactions on Automatic Control, vol. 22, no. 2, pp. 212–222, 1977.

[26] C. J. Fallaha, M. Saad, H. Y. Kanaan, and K. Al-Haddad, "Sliding-mode robot control with exponential reaching law," IEEE Transactions on Industrial Electronics, vol. 58, no. 2, pp. 600–610, 2011.

[27] K. B. Devika and S. Thomas, "Sliding mode controller design for mimo nonlinear systems: A novel power rate reaching law approach for improved performance," Journal of the Franklin Institute, vol. 355, no. 12, pp. 5082–5098, 2018.

[28] S. Yu, X. Yu, B. Shirinzadeh, and Z. Man, "Continuous finite-time control for robotic manipulators with terminal sliding mode," Automatica, vol. 41, no. 11, pp. 1957–1964, 2005.
[29] M. Roopaei and M. Z. Jahromi, "Chattering-free fuzzy sliding mode control in mimo uncertain systems," Nonlinear Analysis: Theory, Methods & Applications, vol. 71, no. 10, pp. 4430–4437, 2009.
[30] K. B. Devika and S. Thomas, "Power rate exponential reaching law for enhanced performance of sliding mode control," International Journal of Control, Automation and Systems, vol. 15, no. 6, pp. 2636–2645, 2017.
[31] R. Kianfar, B. Augusto, A. Ebadighajari, U. Hakeem, J. Nilsson, A. Raza, R. S. Tabar, N. V. Irukulapati, C. Englund, P. Falcone et al., "Design and experimental validation of a cooperative driving system in the grand cooperative driving challenge," IEEE Transactions on Intelligent Transportation Systems, vol. 13, no. 3, pp. 994–1007, 2012.
[32] J. Ploeg, D. P. Shukla, N. van de Wouw, and H. Nijmeijer, "Controller synthesis for string stability of vehicle platoons," IEEE Transactions on Intelligent Transportation Systems, vol. 15, no. 2, pp. 854–865, 2013.
[33] S. Öncü, J. Ploeg, N. Van de Wouw, and H. Nijmeijer, "Cooperative adaptive cruise control: Network-aware analysis of string stability," IEEE Transactions on Intelligent Transportation Systems, vol. 15, no. 4, pp. 1527–1537, 2014.
[34] H. Xing, J. Ploeg, and H. Nijmeijer, "Padé approximation of delays in cooperative ACC based on string stability requirements," IEEE Transactions on Intelligent Vehicles, vol. 1, no. 3, pp. 277–286, 2016.
[35] L. Xu, W. Zhuang, G. Yin, and C. Bian, "Stable longitudinal control of heterogeneous vehicular platoon with disturbances and information delays," IEEE Access, vol. 6, pp. 69 794–69 806, 2018.
[36] Y. Abou Harfouch, S. Yuan, and S. Baldi, "An adaptive switched control approach to heterogeneous platooning with intervehicle communication losses," IEEE Transactions on Control of Network Systems, vol. 5, no. 3, pp. 1434–1444, 2017.
[37] L.-y. Xiao and F. Gao, "Effect of information delay on string stability of platoon of automated vehicles under typical information frameworks," Journal of Central South University of Technology, vol. 17, no. 6, pp. 1271–1278, 2010.
[38] L. Xiao and F. Gao, "Practical string stability of platoon of adaptive cruise control vehicles," IEEE Transactions on Intelligent Transportation Systems, vol. 12, no. 4, pp. 1184–1194, 2011.
[39] S. Darbha, S. Konduri, and P. R. Pagilla, "Benefits of v2v communication for autonomous and connected vehicles," IEEE Transactions on Intelligent Transportation Systems, vol. 20, no. 5, pp. 1954–1963, 2018.
[40] J. Larson, K.-Y. Liang, and K. H. Johansson, "A distributed framework for coordinated heavy-duty vehicle platooning," IEEE Transactions on Intelligent Transportation Systems, vol. 16, no. 1, pp. 419–429, 2014.
[41] A. Alam, B. Besselink, V. Turri, J. Mårtensson, and K. H. Johansson, "Heavy-duty vehicle platooning for sustainable freight transportation: A cooperative method to enhance safety and efficiency," IEEE Control Systems Magazine, vol. 35, no. 6, pp. 34–56, 2015.
[42] V. Turri, B. Besselink, and K. H. Johansson, "Cooperative look-ahead control for fuel-efficient and safe heavy-duty vehicle platooning," IEEE Transactions on Control Systems Technology, vol. 25, no. 1, pp. 12–28, 2016.
[43] R. Rajamani, Vehicle dynamics and control. Springer Science & Business Media, 2011.
[44] H. Pacejka, Tire and vehicle dynamics. Elsevier, 2005.
[45] N. Sridhar, K. V. Subramaniyam, S. C. Subramanian, G. Vivekanandan, and S. Sivaram, "Model based control of heavy road vehicle brakes for active safety applications," in 2017 14th IEEE India Council International Conference (INDICON). IEEE, 2017, pp. 1–6.
[46] L. Davis, "Stability of adaptive cruise control systems taking account of vehicle response time and delay," Physics Letters A, vol. 376, no. 40-41, pp. 2658–2662, 2012.
[47] W. Gao and J. C. Hung, "Variable structure control of nonlinear systems: A new approach," IEEE Transactions on Industrial Electronics, vol. 40, no. 1, pp. 45–55, 1993.
[48] J. Lam, "Model reduction of delay systems using padé approximants," International Journal of Control, vol. 57, no. 2, pp. 377–391, 1993.
[49] V. L. Kharitonov, "The asymptotic stability of the equilibrium state of a family of systems of linear differential equations," Differentsial'nye Uravneniya, vol. 14, no. 11, pp. 2086–2088, 1978.
[50] L. Xu, G. Yin, H. Zhang et al., "Communication information structures and contents for enhanced safety of highway vehicle platoons," IEEE Transactions on Vehicular Technology, vol. 63, no. 9, pp. 4206–4220, 2014.
[51] The Gazette of India, "Fitment of vehicle location tracking device and panic buttons, No. RT-11028/12/2015-MVL, Ministry of Road Transport and Highways, Government of India," 2016.

K. B. DEVIKA (MEMBER, IEEE) received the bachelor's degree in electrical and electronics engineering from Mahatma Gandhi University in 2010, the master's degree in guidance, navigation and control from the University of Kerala, and the Ph.D. degree in control systems from the National Institute of Technology, Calicut, in 2017. She is currently a Post-Doctoral Fellow with the Department of Engineering Design, IIT Madras, India. Her research interests include control of automotive and aerospace systems and sliding mode control.

G. ROHITH (MEMBER, IEEE) received his Bachelor's degree and Master's degree in Applied Electronics and Instrumentation from Calicut University and University of Kerala, respectively, and Ph.D. degree in Aerospace Engineering from Indian Institute of Technology, Madras in 2020. He is currently a Post-Doctoral Fellow with the Department of Mechanical Engineering, Indian Institute of Technology, Gandhinagar, India. His research interests include dynamics and control of automotive and aerospace systems, and multi agent robotics.

VENKATA RAMANI SHREYA YELLAPANTULA received her Bachelor of Technology (B. Tech.) in Mechanical Engineering from SASTRA University, Thanjavur, in 2015. She is currently pursuing Ph. D. in Vehicle Dynamics and Controls in the Department of Engineering Design at Indian Institute of Technology Madras, Chennai, India. Her research interests include, control of automotive systems, Advanced Driver Assistant Systems for heavy road vehicles, and connected vehicles.

SHANKAR C. SUBRAMANIAN (SENIOR MEMBER, IEEE) received the B.E. degree in mechanical engineering from Motilal Nehru Regional Engineering College, Allahabad, India, and the M.S. and Ph.D. degrees from Texas A&M University, USA. He is currently a Professor and a V. Ramamurti Faculty Fellow with the Department of Engineering Design, IIT Madras, Chennai, India. His research interests include dynamics and control with applications to automotive and transportation systems.